Ministry of Higher Education and Research

Scientist

Ibn Khaldoun University – Tiaret –

Faculty of Material Sciences

كـــلية علـــوم المـــــادة

Department of Physics

قسم الفيزياء

Final year project: To obtain the diploma of

Master

Sector : Physics

Specialty : Physics medical

Presented by: TRAWRE SAMBA Bacari

Subject:

Study of the structural and vibrational properties of artemisinin as an antimalarial and hypoglycemic molecule

Supported on: 23/06/2025, In front of the jury:

M.DEBDAB Mansour	**President**	**Prof.**	**Ibn Khaldoun University.Tiaret**
M.MOUMENE Taqyieddine	**Examiner**	**Prof.**	**Ibn Khaldoun University.Tiaret**
Mme DRISSI Mokhtaria	**Examiner**	**Prof.**	**Ibn Khaldoun University.Tiaret**
M.BELARBI El Habib	**Supervisor**	**Prof.**	**Ibn Khaldoun University.Tiaret**
M.MAHFOUD Mohamed	**Co-supervisor**	**MCB**	**Ibn Khaldoun University.Tiaret**

Academic year 2024-2025

Remerciements

Avant tout, nous remercions ALLAH pour le souffle de vie et pour avoir permis la réalisation de ce modeste travail.

➢ *j' exprime ma gratitude au gouvernement algérien, à travers le ministère de l'Enseignement supérieur, ainsi qu'à l'université Ibn Khaldoun de Tiaret, qui, par le biais de leur bourse, m'ont offert la possibilité de suivre ma formation dans les meilleures conditions.*

Mes remerciements vont également à l'ensemble du corps technique et administratif de l'université Ibn Khaldoun de Tiaret.

Nous remercions tout particulièrement :

➢ *Monsieur DEHBI Abdelkader, Doyen, et Monsieur OUARAB Bouakeur, Vice-doyen de la faculté des Sciences de la Matière (SM),*

➢ *Monsieur TRARI Benaissa, le Chef du département de physique,*

➢ *Monsieur BELARBI El Habib, et Monsieur Mahfoud Mohamed, pour leurs orientations, leurs encadrements et pour m'avoir permis de travailler sur ce projet,*

➢ *Monsieur Halis Ladjel, responsable de spécialité Physique Médicale,*

➢*Madame seraisseuret Monsieur DEBDAB Amar du service de la scolarité* et *Madame Hadjira du rectorat, ainsi que les techniciennes et ingénieurs des laboratoires de physique.*

Je tiens à exprimer ma profonde gratitude à Monsieur MOUMENE Taqyieddine, Madame DRISSI Mokhtaria et aux membres du jury, pour le temps et l'attention qu'ils ont consacrés à l'évaluation de ce travail. Je remercie tout particulièrement Monsieur DEBDAB Mansour., président du jury, pour son engagement et ses précieux conseils.

Dédicace

Je rends tout d'abord grâce à Dieu, Le Tout-Puissant, pour m'avoir accordé la force, la patience et la santé nécessaires à la réalisation de ce travail.

Je dédie ce mémoire à mes parents, Monsieur ***BACARI Trawré*** *et Madame* ***KHADY Ba****, ma chère mère qui m'a porté durant neuf mois et qui n'a jamais cessé de m'entourer de son amour, de ses prières et de son soutien inconditionnel. À vous deux, qui avez toujours cru en moi et m'avez transmis les valeurs du courage, de la persévérance et de l'humilité, je vous adresse toute ma gratitude et mon affection la plus sincère.*

Je dédie également ce mémoire à la mémoire de ma petite sœur bien-aimée, ***MAMA Trawré****, partie trop tôt. Que ce travail soit un hommage à son souvenir, à sa lumière, et à l'amour éternel que je lui porte.*

Mes remerciements les plus chaleureux vont également à Mesdames ***KINÉ Gaye*** *et* ***COUMBA Trawré****, qui m'ont toujours entouré d'un amour maternel, d'une bienveillance et d'un soutien précieux tout au long de mon parcours.*

J'exprime aussi ma profonde reconnaissance à mes grands frères ***Malick N'diaye,WOLO Trawré*** *et* ***DEMBA Trawré****, pour leur présence constante, leurs conseils et leur appui moral inestimable.*

Je remercie sincèrement mes meilleurs amis ***BOUBA****,* ***BILAL, GUISSÉ*** *et* ***AMAN****, pour leur fidélité, leur écoute et leur soutien, qui m'ont été d'un grand réconfort durant les moments les plus exigeants de cette formation.*

Je tiens à adresser ma plus vive gratitude à Madame ***FATIMA Mokkdem****, ma professeure, pour sa bienveillance, sa disponibilité et son rôle déterminant dans mon intégration. Son accompagnement et ses encouragements ont été essentiels dans mon cheminement.*

Enfin, mes sincères remerciements vont aux élèves de la spécialité ***Physique Médicale****, qui m'ont accueilli chaleureusement et ont facilité mon intégration avec générosité et solidarité. Leur soutien m'a profondément touché.*

Tables of matters

Summary

Summary

Abstract

Artemisinin, a molecule extracted from Artemisia annua, is widely praised for its effectiveness against malaria. However, recent research has indicated a possible hypoglycemic effect, sparking growing interest in exploring its interactions with biomolecules related to glucose metabolism. The objective of this study is to characterize, through theoretical modeling, the structural, electronic, and vibrational characteristics of artemisinin, as well as its interactions with iron (II) (Fe^{2+}) and glucose. The study was conducted using density functional theory (DFT) via Gaussian09 and GaussView6.0 software. Optimized geometries, frontier orbital energy levels (HOMO-LUMO), vibrational frequencies, and electrostatic potential surfaces were analyzed for isolated molecules and complexes formed. The results show that artemisinin interacts effectively with Fe^{2+}, particularly at the endoperoxide group, supporting its mechanism of action against malaria. Furthermore, the interaction with glucose reveals stable hydrogen bonds, indicating a structural affinity favorable to a hypoglycemic effect. These results shed new light on the therapeutic versatility of artemisinin and open up exciting prospects for the development of compounds with dual antimalarial and antidiabetic activity.

Keywords: artemisinin, malaria, hypoglycemia, glucose, iron (II), DFT, molecular modeling

ملخص

ذلك، ومع .الملاريا مكافحة في لفعاليته واسعة بشهرة يحظى الحولي، الشيح نبات من مستخلص جزيء وهو الأرتيميسينين، الجزيئات مع تفاعلاته باستكشاف متزايدًا اهتمامًا أثار مما الدم، لسكر الخافض تأثيره احتمال إلى الحديثة الأبحاث أشارت والاهتزازية والإلكترونية البنيوية الخصائص توصيف إلى الدراسة هذه تهدف .الجلوكوز بأيض المرتبطة الحيوية الدراسة أُجريت .النظرية النمذجة خلال من والجلوكوز، (Fe^{2+}) الثنائي الحديد مع تفاعلاته إلى بالإضافة للأرتيميسينين، المُحسّنة، الهندسية الأشكال تحليل وتم .GaussView6.0و Gaussian09 برنامجي عبر (DFT) الوظيفية الكثافة نظرية باستخدام للجزيئات الكهروستاتيكي الجهد وأسطح الاهتزازية، والترددات، (HOMO-LUMO) الحدودية المدارات طاقة ومستويات الإيندوبيروكسيد، مجموعة في وخاصةً ،Fe^{2+} مع بفعالية يتفاعل الأرتيميسينين أن النتائج تُظهر .المُشكّلة والمعقدات المعزولة مما مستقرة، هيدروجينية روابط عن الجلوكوز مع التفاعل يكشف ذلك، على علاوة .الملاريا مكافحة في عمله آلية يدعم مما للأرتيميسينين، العلاجي التنوع على جديدًا ضوءًا النتائج هذه تُلقي .الدم لسكر خافض تأثير إلى يُفضي هيكلي تقارب إلى يشير .للسكري ومضاد للملاريا مضاد مزدوج نشاط ذات مركبات لتطوير للاهتمام مثيرة آفاقًا وتفتح

المفتاحية الكلمات : الحديد الجلوكوز، الدم، سكر نقص الملاريا، الأرتيميسينين،

الهيدرو الرابطة الجزيئية، النمذجة ،DFT ،(II)

Résumé

L'artémisinine, molécule extraite de l'Artemisia annua, est largement saluée pour son efficacité contre le paludisme. Cependant, des recherches récentes ont indiqué un possible effet hypoglycémiant, suscitant un l'intérêt croissant d'explorer ses interactions avec des biomolécules liées au métabolisme du glucose. L'objectif de cette étude vise à caractériser, à travers une modélisation théorique, les caractéristiques structurales, électroniques et vibratoires de l'artémisinine, ainsi que ses interactions avec le fer (II) (Fe^{2+}) et le glucose. L'étude a été réalisée en utilisant la théorie de la fonctionnelle de la densité (DFT) via les logiciels Gaussian09 et GaussView6.0. Les géométries optimisées, les niveaux d'énergie des orbitales frontières (HOMO-LUMO), les fréquences vibrationnelles et les surfaces de potentiel électrostatique ont été analysés pour les molécules isolés et les complexes formés. Les résultats montrent que l'artémisinine interagit efficacement avec Fe^{2+}, particulièrement au niveau du groupement endoperoxyde, ce qui soutient son mécanisme d'action contre le paludisme. De plus, l'interaction avec le glucose met en évidence des liaisons hydrogène stables, ce qui indique une affinité structurelle favorable à un effet hypoglycémiant. Ces résultats apportent un éclairage nouveau sur la polyvalence thérapeutique de l'artémisinine et ouvrent des perspectives intéressantes pour le développement de composés à double activité, antipaludique et antidiabétique.

Mots-clés: artémisinine, paludisme, hypoglycémie, glucose, fer (II), DFT, modélisation moléculaire

List of abbreviations

A. annua: Artemisia annua

ART: Artemisinin

ADF: Amsterdam Density Functional

B3LYP: Becke 3-parameter -Lee, Yang and Parr

DOS: Density Of States

DDE: Dynamic Data Exchange

ESP: Electrostatic Potential

GGA: Generalized Gradient Approximation

GTOs: Gaussian-Type Orbitals

Glc: Glucose

HOMO: Highest Occupied Molecular Orbital

HFR: Hartree Fock-Roothaan

HF: Hartree Fock

IgE: Immunoglobulin E

Freq: Frequence

LUMO: Lowest Unoccupied Molecular Orbital

NF-KB: Nuclear Factor Kappa B

OLE: Object Linking and Embedding

OA: Orbital Atomic

OPT: Optimization

PDB: Protein Data Bank

PADH: Post-artesunate delayed hemolysis

PI3K: Phosphatidylinosito-3-kinase

SCF: Self consistent field

STOs: Slater Type Orbitals

List of figures

List of figures

List of tables

GENERAL INTRODUCTION

General introduction

The plant *Artemisia annua* has a bioactive molecule called artemisinin, which has been used for centuries in traditional Chinese medicine to treat feverish states. Its discovery as an antipaludic drug in the 20th century marked a turning point in the fight against paludism, a parasitic disease that still threatens millions of lives worldwide, especially in tropical and subtropical regions. However, in addition to its role in the fight against paludism, recent research indicates that artemisinin may also have hypoglycemic properties, opening the door to potential other pharmacological uses, such as the treatment of type 2 diabetes. This diversity of therapeutic applications highlights the importance of an in-depth knowledge of the relationship between the molecular structure of artemisinin and its biological properties. Such knowledge is crucial to direct the rational development of more efficient and selective derivatives.

Although the efficacy of artemisinin is widely recognized, in-depth knowledge of its mechanisms of action at the molecular level remains incomplete, particularly with respect to its essential physicochemical properties. In addition, the latest studies on its hypoglycemic properties suggest that interaction mechanisms have not yet been discovered, which require an in-depth analysis of its structure and electronic behavior.

Thus, a crucial question arises: How might a study of artemisinin's structural, vibrational, and electronic characteristics help us better understand its antipaludic mechanisms of action and emerging hypoglycemic effects?

The purpose of this study is to better understand the molecular interactions of artemisinin by optimizing the molecule and analyzing its physicochemical properties.

The main objective revolves around two points:

a) To improve the molecular structure of artemisinin through numerical modelling techniques;
b) Evaluate and examine its essential characteristics such as molecular vibrations, energy levels of boundary orbitals (HOMO, LUMO, ESP, DOS), as well as other crucial electronic parameters.

This study will make it possible to make a precise link between the structure of artemisinin and its biological properties, with a view to the future development of new molecules for a wider therapeutic range.

Part I:Bibliography

Synthesis

CHAPTER I:

LITERATURE REVIEW

Part I: Bibliography synthesis

Chapter I: Literature review

1. HISTORICAL OVERVIEW OF ARTEMISININ

1.1 Introduction

The discovery of artemisinin for malaria therapy by Chinese scientists in the 1970s was one of the greatest discoveries in medicine in the 20th Century; however, the history of its discovery has been a mystery and even controversial. While this subject has been discussed in several reviews, a recently published book entitled A Detailed Chronological Record of Project 523 and the Discovery and Development of Qinghaosu (Artemisinin), edited by Jianfang Zhang and six other scientists who participated in the project, provides a more detailed account **[L. Cui and.,2009][1].**

1.2 Artemisinin

Artemisinin (Figure 1) is a sesquiterpene lactone, incorporating an endoperoxide group. As the active component of Artemisia annua L., it was first isolated and identified by Chinese scientists in 1970s.Pharmacological experiments have shown that artemisinin and its derivatives not only can be used to treat malaria, but also has other pharmacological functions, such as antioxidant, antitumor, antiarrhythmic, anti-fibrosis, regulation of the body's immune, and the activity against schistosomiasis **[F. Liao,2009] [2].**

2. CHEMICAL AND THERAPEUTIC OF ARTEMISININ PROPERTIES

2.1 Chemical properties

Artemisinin has poor solubility in either water or oil, and instead, it is soluble in many aprotic solvents. In contrast to the general concept that molecules containing endoperoxides are susceptible to decomposition, artemisinin is amazingly thermostable; even when the temperature reaches its melting point at about 156-157 °C, no obvious decomposition is

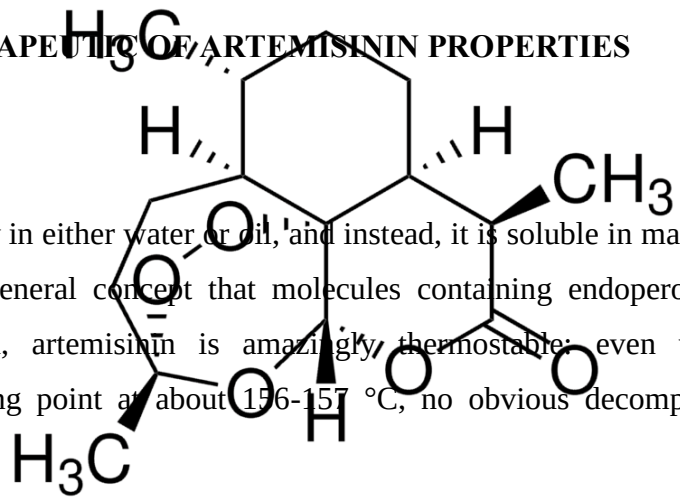

Figure I-1:Artemisinin

*[***Source: Sigma,2009** *http://www.sigmaaldrich.com/]*

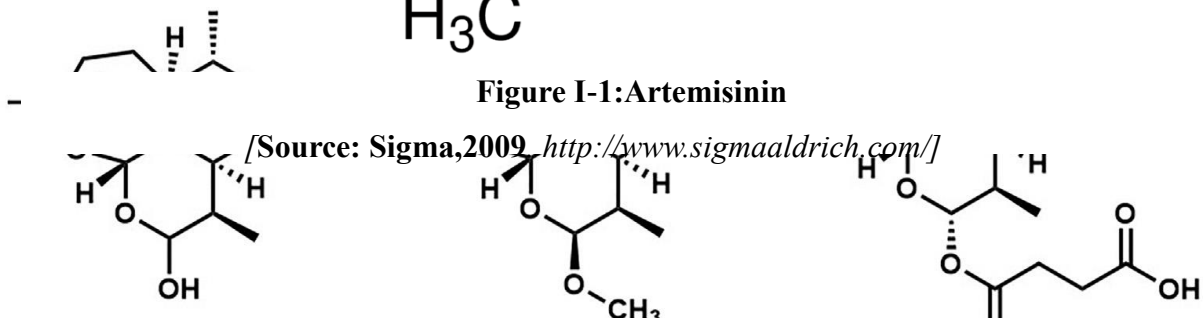

Figure I-2: Structure derivates of artemisinin

observed. However, further temperature increases to 190 °C leads to the breakdown of this molecule. The carbonyl group of artemisinin was reduced to obtain DHA(Dihydroartemisimin) and its derivatives such as the water-soluble artesunate and oil-soluble artemether [**J. Li and al., 2010][3].**

2.2 Therapeutic properties

2.2.1 Antimalarial effect of artemisinin

Artemisinin is among the most potent antimalarial agents, effective against nearly all asexual and sexual parasite stages. They can kill malaria parasites within minutes with a parasite reduction ratio of approximately 10,000 per erythrocytic cycle, resulting in rapid clinical responses (**M. Xia and., al 2020) [4].**

2.2.2 Anti-Inflammation effect of artemisinin

Inflammation plays a pivotal role in the pathophysiological processes of kidney diseases and associated with renal injury . The anti-inflammatory effects of artemisinin have been widely recognized, including repression of nuclear factor-kB (NF-kB), toll-like receptors (TLRs), signal transducer and activator of transcription (STAT), and phosphatidylinositol-3- kinase (PI3K)/protein kinase B (AKT) activity , which are key factors mediating immune-inflammatory response and are associated with kidney disease progression **[C. Shi and al., 2015][5].**

2.2.3 Artemisinin derivatives treat allergic diseases

Allergy is an acquired hypersensitivity reaction of the immune system mediated by cross-linking of allergen-specific IgE with high affinity IgE receptors, leading to immediate mast cell degranulation. Allergic disorders have substantially different pathogenesis with autoimmune diseases. However, artemisinin derivatives were also reported to be therapeutic against the allergic diseases **[A. I. Alagbonsi and al., 2025][6].**

2.2.4 Antidiabetic effect of artemisinin

Artesunate (derivate of artemisinin) include reduced reticulocytes and post-artesunate delayed hemolysis (PADH). On glucose homeostasis, a recent report showed the hypoglycemic and

antidiabetic effects of Artemisia annua, the plant from which artemisinin was made. In addition, the antidiabetic property of other artemisia plants has also been reviewed. As an artemisinin derivative, information on the effect of artesunate on glucose homeostasis is still scanty. Artesunate and other artemisinin have been shown to cause hypoglycemia, increased glucose-6-phosphate dehydrogenase activity, as well as the conversion of pancreatic a-cells to insulin-secreting b-like cells **[L. Ilham, 2025][7].**

2.2.5 Treatment of skin diseases effect of artemisinin

In clinical applications, artemisinin and its derivatives have been shown to be safe in the treatment of connective tissue diseases such as dermatitis (eczema), photosensitive dermatosis, summer vesicle disease, psoriasis vulgaris, and dermatomyositis. Studies have shown that artemisinin and its derivatives are effective in the treatment of certain skin diseases. For example, the efficacy rate of artesunate in treating eczema was 100%, and the efficacy rate in treating pleomorphic erythema, pleomorphic solar rash, and summer vesicles was 100%. Efficacy rates for the treatment of psoriasis vulgaris and dermatomyositis were 60% and 75%, respectively **[Y. Huang and al., 2023][8].**

3. *ARTEMESIA* SPECIES: SOURCE AND EXTRACTION

3.1 Source

Artemisia is a wild and perennial plant, it is a Mediterranean and Saharan-Indian species, grows in the high steppe plains. Also known as desert wormwood, it grows in arid or semi-arid lands (MESSAI, 2015, p. 46), as its growth differs from one region to another in the regions of Aures, whether mountainous, plain, or desert (HOUMANI, 2004, p. 165). Go into this Sen by saying that it develops in clayey steppes or in humid places. Its development is related to the nature of the soil, and being in rural areas, and widely consumed by cattle, it is also considered an antiseptic, where in the mountainous regions of the aures with solid soil, while in the desert side it is soft, sandy or semi-sandy **[M. Merradi and al., 2021][9].**

3.1.1 The genus *Artemisia*

The genus *Artemisia* contains artemisinin, a drug substance against malaria, isolated from the Chinese plant *Artemisia annua*. Artemisinin, which is a sesquiterpene lactone, is not the only drug component in this genus, there are other sesquiterpene lactones,10 sesquiterpene lactones

and flavonoids that are used with a low risk of toxicity. Along with other species of this genus, we find the *Artemisia* herba alba Asso [**LAMARI, 2018][10].**

Artemisia belongs to the important family Asteraceae, one of the largest families, which comprise about 1,000 genera and more than 20,000 species. Within this family, *Artemisia* encompasses more than 500 species. It is characterized by a wide range of morphological and phytochemical variability, which is associated with different geographical origins of the samples (Bora & Sharma, 2011) [**M. J. Abad and al., 2012][11].**

3.1.2 Morphological description

Under a whitish tomentose shrub, 30 to 50 cm, with numerous erect stems, woody at the base; leaves pubescent, divided into small, thin silvery-green strips; inflorescences very small, yellowish, sessile, grouped by 2 to 12 (depending on the variety); bracts of the involucre glandular, characteristic aromatic odor [**Ozenda P., 1983][12].**

Figure I-3: ***Artemisia compestris***

*[***Source : Battandier, J.A and L.C. Trabut (1889***). https://efloramaghreb.org/specie/135951]*

3.1.3 Pharmacological activities

The genus *Artemisia* has been the subject of numerous scientific studies involving Evidence of various activities. Artemisia species are frequently used for the treatment of diseases such**[Abad M.J. and al., 2012][11].**

- *Artemisia* absinthium L. is used for its antiparasitic effects and to treat anorexia and indigestion. The aerial parts are present in many preparations based on gastric plants, food supplements and alcoholic beverages;
- *A*. afra is used for many ailments, including colds, coughs, diabetes, heartburn, and asthma,
- *A. annua* L. is used as a tea for the treatment of malaria;
- campestris L. has a wide range of antimicrobial, anti-inflammatory and anti-venom properties;
- *A*. herba alba Asso is used as a decoction against fever and menstrual and nervous problems;
- *A.* vulgaris L is widely used for its antihypertensive, anti-inflammatory, antispasmodic, carminative and deworming actions

3.1.4 Plant systematics

Kingdom: Plantae

Phylum: Spermaphytes (Phanerogams) or "seed plants"

Subphylum: Angiosperms (Flowering plants)

Class: Dicotyledons (Magnoliopsida)

Subclass: Asteridae

Order: Asterales

Family: Asreraceae

Figure I-4:*Artemisia* **herba alba Asso**

Tribe: Anthemideae

Subtribe: Aremisiinae

Genus: *Artemisia*

[**Source : Floratrek**,, **2013**.*https://commons.wikimedia.org]*

Species: *Artemisia* herba alba Asso

[**Guignard J.L., 199][13].**

3.1.5 Geographical description

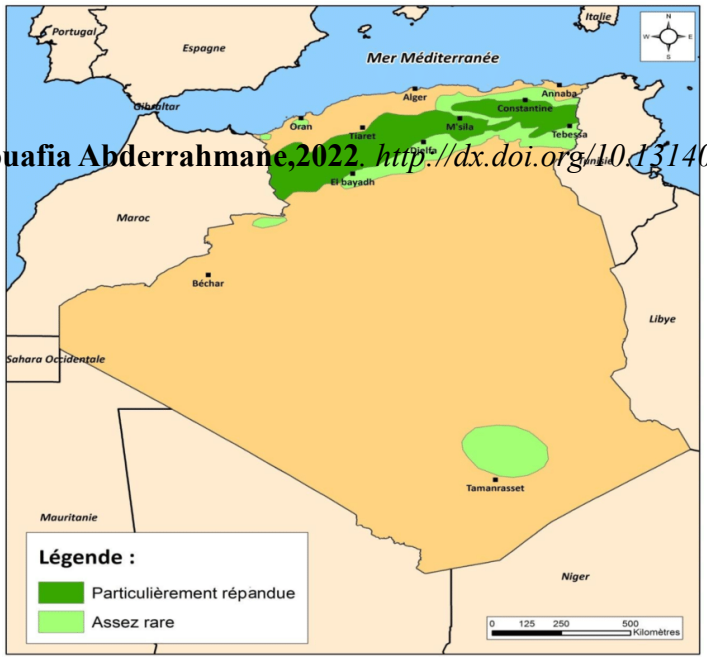

[**Source : Bouafia Abderrahmane,2022**. *http://dx.doi.org/10.13140/RG.2.2.21876.42880]*

3.1.6 Traditional medicine

Artemisia, also known as desert wormwood, is a mainly forage plant, much appreciated by livestock as winter. This species has been used in traditional medicine by many cultures since ancient times for its stomachic,

Figure I-5: Geographical description of *artemisia* herba alba Asso

antispasmodic, antigastralgic, deworming actions…….. [**Messai L., 2011] [14].**

3.2 Extraction of artemisinin

3.2.1 Extraction by conventional methods

well-established procedure for extracting artemisinin from its plant source (A. annua) involves soaking in nonpolar organic solvents such as hexane or petroleum ether under reflux conditions . However, despite the high solubility of artemisinin in these solvents, extraction is still not very specific because other compounds are also present in crude extracts, such as: essential oils, chlorophylls, terpenes, sugars, artemisinin derivatives, and long-chain nonpolar lipids . The latter group, called waxes, is the main group of compounds in these extracts and is present due to the extraction of the protective layer on the surfaces of the leaves. These waxes are largely composed of hydrocarbons and aliphatic alcohols . It has been noted that these waxy impurities contribute to the overall low extraction yield of artemisinin, as isolation of artemisinin from these impurities is difficult due to the high solubility of artemisinin in waxes [**A. A. Lapkin and al., 2010][15].**

The more impurities the crude extracts contain, the more expensive purification becomes, making artemisinin-based drugs, such as antimalarial artemisinin-based combination therapies (ACTs), more expensive.

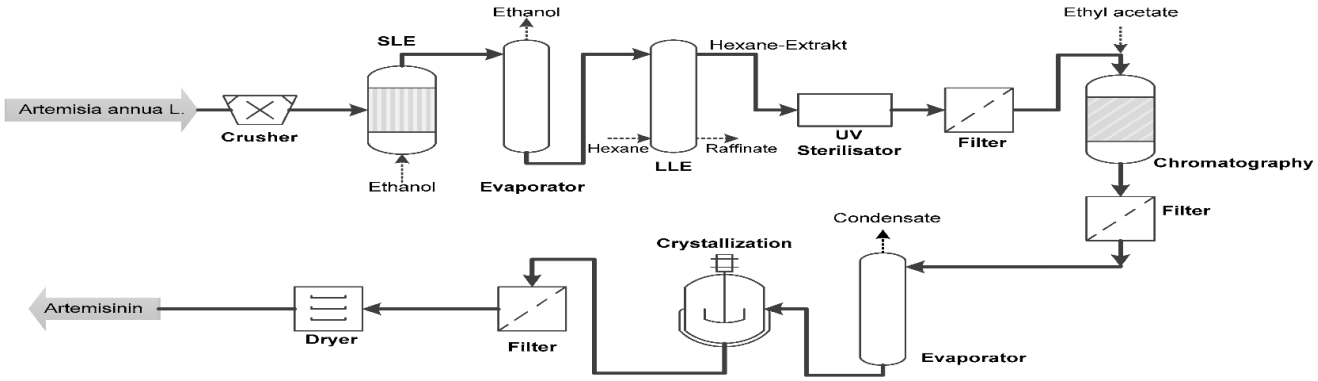

*[**Source** : **Maximilien Sixt,2018**. https://doi.org/10.5590/pr6090161]*

Since extraction from *A. annua* is currently the only realistic source of artemisinin, it is imperative to improve the efficiency of artemisinin extraction. This need is reinforced by the fact that the artemisinin content in *A. annua* is very low with a concentration of around 0.01 to 1.4% and currently the amount of artemisinin extracted by conventional methods is only 60 to 80% **[Briars and Larysa Paniwnyk., 2013][16].**

Figure I-6: Flow scheme of the benchmark process, (SLE, solid-liquid extraction; ultraviolet).

3.2.2 Extraction by ultrasound

One of the potential methods to improve the efficiency of artemisinin extraction is the use of ultrasound. The fundamental theory of ultrasonic activity is based on the cavitation bubbles formed by the force radiated by the rarefaction steps of ultrasonic waves. These bubbles produce "micro-jets" when they collapse abnormally near surfaces present in a "heterogeneous system". These forces are powerful enough to form fissions in cell walls, facilitating the movement of the solvent and the release of components from cells and trichome glands . Artemisinin would thus be more easily accessible and, therefore, easier to extract, thanks to the use of ultrasound **[R. Briars and Larysa Paniwnyk., 2013][17].**

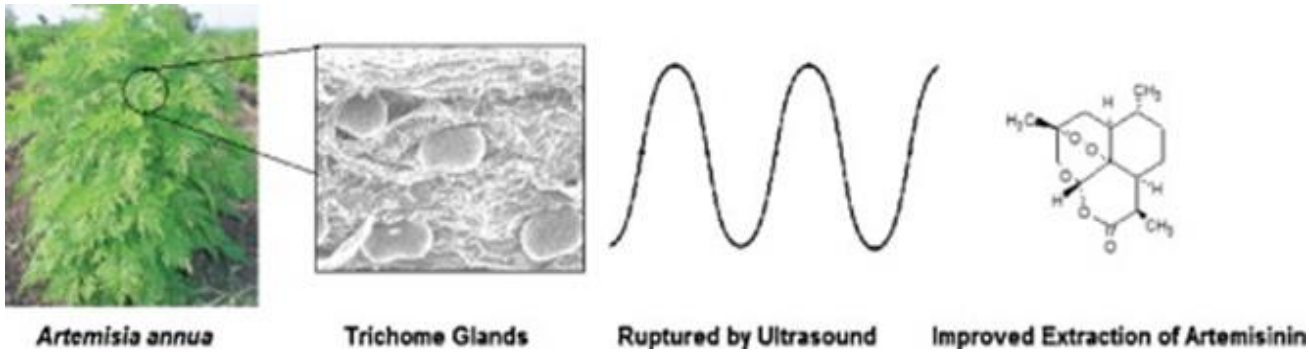

Figure I-7: Extraction by ultrasound

*[***Source***:* **Rhianna Briars and Larysa Paniwnyk***,* **2013.***https://doi.org/10.1016/j.indcrop.2012.06.043]*

4. COMPUTATIONAL METHODS IN MOLECULAR CHARACTERIZATION

4.1 Quantum mechanics

Quantum mechanics is the fundamental physical theory that describes the behavior of matter and of light; its unusual characteristics typically occur at and below the scale of atoms. It is the foundation of all quantum physics, which includes quantum chemistry, quantum field theory, quantum technology, and quantum information science… . **[18].**

4.2 Molecular mechanic

Molecular mechanics is a method called the force field method, which is the latter is a mathematical model based on the fundamental principles of spectroscopy Vibrational; potential energy is described as steric energy; for a molecule its value depends on the force field adopted.

This energy is expressed as a sum of contributions associated with deviations of the structure from the reference parameters (bond length, valence angle,) and a sum of characteristic 3D contributions steric energy (Van der Waals energy, Coulomb energy, ...) **[18].**

4.3 Molecular dynamic

Molecular dynamics is a computer modeling technique by in which the evolution as a function of time or trajectory, of a molecule is described by the principles of classical Newtonian mechanics. In molecular dynamics, we try to simulate intramolecular movements which can then be viewed in real time. These movements correspond to vibrations around a minimum or the transition from one minimum to another minimum of energy. If the energy virtually supplied to the system is sufficiently high, energy barriers can be crossed **[19].**

References Bibliography

[1] **L. Cui and X. Su**, "*Discovery, mechanisms of action and combination therapy of artemisinin," Expert Rev. Anti Infect. Ther., vol. 7, no. 8, pp. 999–1013, Oct. 2009, doi: 10.1586/eri.09.68.*

[2] **F. Liao**, *"Discovery of Artemisinin (Qinghaosu)," Molecules, vol. 14, no. 12, pp. 5362–5366, Dec. 2009, doi: 10.3390/molecules14125362.*

[3] **J. Li and B. Zhou**, *"Biological Actions of Artemisinin: Insights from Medicinal Chemistry Studies," Molecules, vol.15, no.3, pp.1378–1397, Mar.2010, doi:10.3390/molecules15031378.*

[4] **M. Xia, D. Liu, Y. Liu, and H. Liu**, *"The Therapeutic Effect of Artemisinin and Its Derivatives in Kidney Disease," Front. Pharmocol., vol. 11, p. 380, Mar. 2020, doi: 10.3389/fphar.2020.00380.*

[5] **C. Shi, H. Li, Y. Yang, and L. Hou**, *"Anti-Inflammatory and Immunoregulatory Functions of Artemisinin and Its Derivatives," Mediators Inflamm., vol. 2015, no. 1, p. 435713, Jan. 2015, doi: 10.1155/2015/435713.*

[6] **A. I. Alagbonsi, T. M. Salman, S. O. Sulaiman, K. A. Adedini, and S. Kebu,** *"Possible mechanisms of the hypoglycemic effect of artesunate: Gender implication," Metab. Open, vol.10, p.100087,2021, Accessed: Feb.22,2025. [Online]. Available: https://www.sciencedirect.com/science/article/pii/S2589936821000116*

[7] **L. Ilham,** *"Effet de l'armoise blanche (Artemisia herba alba Asso) sur les performances zootechniques et la glycémie chez le poulet de chair," 2018, Accessed : Mar. 11, 2025. [Online]. Available: http://archives.univbiskra.dz/bitstream/123456789/11065/1/LAMARI_Ilham.pdf*

[8] **Y. Huang, Y. Yang, G. Liu, and M. Xu,** *"New clinical application prospects of artemisinin and its derivatives: a scoping review," Infect. Dis. Poverty, vol. 12, no. 1, p. 115, Dec. 2023, doi : 10.1186/s40249-023-01152-6.*

[9] **M. Merradi, K. Bouguerra, and S. Bayou**, *"La guérissions à base de l'Armoise blanche en médecine traditionnelle dans les Aurès (Algérie)-Etude anthropologique, vol. 5, no. 2, pp.10651074,2021, Accessed : Feb.22,2025. [Online]. Available : https://asjp.cerist.dz/en/article/170067.*

References Bibliography

[10] LAMARI, *"Effet de l'armoise blanche (Artemisia herba alba Asso) sur les performances zootechniques et la glycémie chez le poulet de chair," 2018, Accessed : Feb. 22, 2025. [Online]. Available : http://archives.univbiskra.dz/bitstream/123456789/11065/1/LAMARI_Ilham.pdf.*

[11] M. J. Abad, L. M. Bedoya, L. Apaza, and P. Bermejo, "*The Artemisia L. genus: a review of bioactive essential oils," Molecules, vol. 17, no. 3, pp. 2542–2566, 2012,* Accessed: Mar. 11, 2025. [Online]. Available : https://www.mdpi.com/1420-3049/17/3/2542.

[12] R. Sihem, *"Efficacité de l'extrait d'Artemisia herba-alba sur le puceron vert du pêcher Myzus persicae, signalé sur Piment cultivé sous serre dans la région de Biskra", Accessed : Mar.13,2025. [Online]. Available: http://archives.univbiskra.dz/bitstream/123456789/22662/1/RAIS_Sihem.pdf.*

[13] Guignard J.L., *1998 : Abrégés botanique. 11e édition. Edition Masson. Pp.49-205).*

[14] Messai L., *2011 : Etude phytochimique d'une plante medicinale de l'Est algérien (Artemisia herba alba). These de Doctorat. Université de Constantine.*

[15] A. A. Lapkin and al., *"Screening of new solvents for artemisinin extraction process using ab initio methodology," Green Chem., vol. 12, no. 2, pp. 241–251, 2010, Accessed: Mar. 11,2025. [Online]. Available : https://pubs.rsc.org/en/content/articlehtml/2010/gc/b922001a.*

[16] R. Briars and L. Paniwnyk, *"Effet des ultrasons sur l'extraction de l'artémisinine de l'Artemisia annua," Ind. Crops Prod., vol. 42, pp. 595–600, Mar. 2013, doi : 10.1016/j.indcrop.2012.06.043.*

[17] Feynman, Richard; Leighton, Robert; Sands, Matthew (*1964***).** *Les conférences Feynman sur la physique . Vol. 3. California Institute of Technology. Consulté le 19 décembre 2020.Réimprimé, Addison-Wesley, 1989, ISBN 978-0-201-50064-6*

[18] N.L. Allinger, X. Zhou, J. Bergsma, J. Mol. Structr. (Theochem), *1994,312, 69.*

[19] J. Tirado-Rives & W.L. Jorgensen, J. Am. Chem. Soc., *1990,1*

CHAPTER II:

THEORETICAL BACKGROUND

Chapter II: Theoretical background

Introduction

Computational quantum chemistry is a branch of theoretical chemistry whose major aim is to make efficient mathematical approximations and computer programs for calculating the properties of the molecules such as their total energy, vibrational frequencies, dipole and quadrupole moments, potential energy (free energy) surfaces, excitation energies, and some other diverse spectroscopic quantities, reactivity behavior, the involved reaction mechanism, and reaction dynamics. The term is sometimes useful in covering the areas of overlap between computer science and chemistry **[1].**

Quantum Chemistry is a very nice tool for studying properties and reactions of molecules. Recently years the quantum chemistry development particularly that of density functional theory (DFT) methods, have made calculations of quantum chemistry more accurate and matching to those of experimental calculations for molecules of moderate sizes.

The quick advancement of computer technology has enormously urged chemists to utilize quantum science for understanding the model and predicting properties and reactions of the molecules, nanometer materials properties, as well the techniques which be used in the biological systems**.**

Mostly these methods include various empirical parameters those are optimized by reproducing properties of some reference molecules and that parameters usually be accurate for the systems that are parameterized for.

For many properties e.g. the relative energies of different conformations of a big molecule, the binding energy, and the hydrogen-bonded system structure. The results from semi-empirical calculations are not trustable, so this limits their applications to large systems, particularly those where hydrogen bonds are significant. In recent years, many quantum chemistry methods introduced specifically for studying large molecular systems **[2].**

1. OVERVIEW OF AB INITIO, DENSITY FUNCTIONAL THEORY (DFT), AND RELATED TECHNIQUES

1.1 Ab initio

Parameters adjusted to the experimental results are not used. The calculations are generally more complex and require large it resources. Calculations ab initio come from either Hartree Fock (and post-Hartree Fock) methods using wave function to describe the quantum system, so be it. those of the theory of which uses the electron density. The main advantage of the DFT is the saving of computation time. Ab initio methods are characterized by the introduction of an arbitrary base to extend the molecular orbitals and then the explicit calculation of all the required integrals that imply this basis **[3].**

1.2 Density Functional Theory (DFT)

In the formalism of the density functional theory, energy is expressed as a function of the electron density. The first to have expressed energy in L.H. Thomas (1927), E. Fermi (1927, 1928) and P.A. Dirac (1930) on the model of the non-interacting electron gas. The purpose of DFT methods is to determine functionals that allow us to give a relationship between the density of the electronics and energy. DFT really started with theorems Hohenberg and Kohn in 1964, which establish a functional relationship between the energy of the ground state and its electron density. The two theorems show the existence of a density functional that allows us to calculate the energy of the ground state of a system **[4].**

The method based on the density functional uses an expression of energy E as a function of the electron density ρ, which in turn is a function of the position of the electron $\vec{r}$

$$\boldsymbol{E = F\,[\rho(\vec{r})]} \qquad \textbf{(II-1)}$$

Energy is therefore a function, i.e. a functional of $\vec{r}$.

Hohenberg and Kohn's theorems: The Density Functional Theory (DFT) is based on the double Hohenberg and Kohn's theorem applies to any N-electron system interacting in an external potential, $V_{ext}(\vec{r})$and whose ground state [**P. Hohenberg and al., 1964**] **[5]**.

Theorem 1:

The first postulate of Hohenberg and Kohn's theorem consists in giving a theoretical justification for the idea that the ground state energy of the of electrons, subjected to an external potential, $V_{ext}\ (\vec{r}\ )$(e.g. the field created by the kernels or an applied field, etc.), is a functional that depends on only of the electron density$\rho(\vec{r})$[**P. Hohenberg and al., 1964**][**5**]**.**

$$\rho(\vec{r}) = N \int \Psi^*(r_1, r_{2,\ldots\ldots}\, r_N)\Psi(r_1, r_{2,\ldots\ldots}\, r_N)dr_1 dr_{2\ldots\ldots}\, dr_N \qquad \textbf{(II-2)}$$

The base variable is now $\rho(\vec{r})$.

Theorem 2:

The exact ground state density for a system is the one that minimizes energy through the functional E[ρ].In addition, the first Hohenberg–Kohn theorem states that for the functional energy of a system in a given external potential $\widehat{V_0}(\vec{r})$:

$$E_{V_0}[\rho] = < \Psi[\rho] \left|\hat{T} + \widehat{V_{ee}} + \hat{V_0}\right| \Psi[\rho] > \qquad \textbf{(II-3)}$$

The exact density of the ground state can be obtained by minimizing $E_{V0}\ [\rho]$:

$$E_0 = min\ E_{V_0}[\rho] \qquad \textbf{(II-4)}$$

The part of the functional energy that is not related to the external potential,$F_{HK}[\rho]$ is a functional universal density.

$$E_{HK}[\rho] = E_{V_0}[\rho] = F_{HK}[\rho] + \int V_0\,(\vec{r})\rho_0(\vec{r})d\vec{r} \qquad \textbf{(II-5)}$$

$$F\ [\rho(r)] = < \Psi[\rho] \left|H - V_{e\chi}\right| \Psi[\rho] > = < \Psi[\rho]\ |T - V_{ee}|\Psi[\rho] > \qquad \textbf{(II-6)}$$

$$F\ [\rho] = T[\rho] + V_{ee}[\rho] \qquad \textbf{(II-7)}$$

With:

$T[\rho]$ is functional of kinetic energy.

$V_{ee}[\rho]$ is functional of the electron-electron interaction.

The total energy of the system is a functional of ρ (r), which is written as:

$$E= E[\rho] = F[\rho] + \int V_{ext}\,(r).\,\rho(r)\,dr \qquad \textbf{(II-8)}$$

1.3 Related techniques

1.3.1 Hyperchem

Hyperchem is a commercial molecular modeling program for Windows that is easily accessible to beginning students. It includes molecular mechanics using several force fields, together with semi-empirical and ab initio quantum mechanical calculations. Molecules may be presented as stick, ball and stick, space-filling, or dotted surface models. Molecular orbitals may be displayed as two-dimensional contour maps or as three-dimensional isodensity surfaces. UV and IR spectra are presented as spectral displays and individual vibrational modes are animated. Hyperchem reads PDB (ENT) files as well as its own HIN format files. One of the strengths of Hyperchem is that it can be driven with internal scripts as well as DDE/OLE interaction with other Windows programs. A freely-distributed web browser plug-in supports manipulable 3-D views of molecules generated by Hyperchem **[6].**

1.3.2 Gaussian

Gaussian is the "industry standard" for ab initio molecular computation of energies, molecular structures, and vibrational frequencies -- along with numerous molecular properties that are derived from these three basic computation types -- for systems in the gas phase and in solution. Additional basis sets and computation types are constantly being added **[7].**

1.3.3 Gaussian view

a full-featured graphical user interface for Gaussian 98 (Unix or Windows). With the molecule building facility one can quickly and efficiently construct molecular systems. Gaussian calculations can be initiated and monitored from the GaussView and when a calculation has completed, we can use GaussView to examine a variety of results graphically via its advanced visualization facilities **[8].**

2. PREVIOUS COMPUTATIONAL STUDIES ON SIMILAR MOLECULES

2.1 Introduction

Artemisinin constitutes the frontline treatment to aid rapid clearance of parasitaemia and quick resolution of malarial symptoms. However, the widespread promiscuity about its mechanism of action is baffling. There is no consensus about the biochemical target of

artemisinin but recent studies implicate haem and PfATP6 (a calcium pump). We investigated the role of iron and artemisinin on PfATP6, in search of a plausible mechanism of action, via density functional theory calculations, docking and molecular dynamics simulations. Results suggest that artemisinin gets activated by iron which in turn inhibits PfATP6 by closing the phosphorylation, nucleotide binding and actuator domains leading to loss of function of PfATP6 of the parasite and its death. The mechanism elucidated here should help in the design of novel antimalarials [**A. Shandilya and., *2013*] [9].**

2.2 Density functional theory (DFT) calculation

The geometries of both artemisinin and the haem group were fully optimized using density-functional theory as implemented in the ADF package 43 and as carried out by Araujo et al. The states with singlet, triplet and quintet multiplicities (S=0, 1 and 2, respectively) were calculated for haem, while triplet, quintet, and septet states (S =1, 2, and 3, respectively) were calculated for the complex between haem and artemisinin. Triple zeta with single polarization (TZP) basis set and PBE functional44 was used. The computed charges on each oxygen atoms are provided in Supplementary Table T1. It was found that for interaction at short distances, due to artemisinin reduction by the haem group, the most stable complex has a septet spin state. Further computational details and the more insight into the interaction of haem and artemisinin can be found in that work. The resulting geometry which was of the same order as in the work of Araujo et al. were used for docking [***A. Shandilya and, 2013]*** **[9].**

Table 1 | Average binding free energies computed from the MD trajectories

Molecule	Target/Enzyme	Binding Free Energy (kcal/mol)
Artemisinin	PfATP6*	−6.5
Fe-artemisinin	PfATP6*	−8.3
Thapsigargin	PfATP6*	−6.7
Artemisinin	Mammalian SERCA (1SU4)	−4.2
Fe-artemisinin	Mammalian SERCA (1SU4)	−5.1
Thapsigargin	Mammalian SERCA (1SU4)	−9.1

*Modelled using 1SU4 as described in text.

Figure II-8: Average blinding free energies computed from the MD trajectories

[Source: A. Shandilya and, 2013. *https://doi.org/10.1038/srep02513]*

2.3 Docking

Docking of artemisinin and Fe-artemisinin adduct to PfATP6 was carried out using Pardock45–49. Scoring of these docked structures was done by Bappl49. Details of the

docking methodology are provided in the supplementary information. These docked structures were taken as input for molecular dynamics simulations [**A. Shandilya and,*2013*][9].**

2.4 Molecular dynamic

All MD simulations were carried out using GROMACS50. Amber FF99SB51 force field was used. The complexes obtained from Pardock were solvated in a box of TIP3P52 water molecules (and 30 counter ions to ensure electroneutrality) and minimized for an additional 2500 steps (1000SD+1500CG). All these systems sizes comprised around, ~275,000 atoms.MD Simulations were started by slowly heating the solvent to 300 K over a period of 100 ps keeping the complex fixed. After this, the entire system was gradually brought to 300 K over a period of 300 ps. The simulation was then carried out under NPT conditions for 100 ns. A 2 femto second time step was used for integrating the equations of motion. Periodic boundary conditions were applied throughout the MD simulations, along with PME summation 53 for treating electrostatics. The temperature was kept constant by coupling heat bath through the Berendsen algorithm54 using separate solute and solvent scaling. Pressure was adjusted by isotropic position scaling using a Berendsen like algorithm. Covalent bonds to hydrogen atoms were constrained by the SHAKE algorithm55. Convergence of energy, density was monitored. The initial 10 ns was treated as equilibration and the subsequent 100 ns was treated as production phase for structural and energy analyses [**A. Shandilya and.,2013**] **[9].**

3. QUANTUM MECHANICAL APPROACHES IN COMPUTATIONAL CHEMISTRY

3.1 Quantum mechanics

Quantum mechanics (QM) is the correct mathematical description of the behavior of the electrons and thus of chemistry. Theoretically, by QM it's possible to predict any property of an individual atom or molecule precisely. Practically, its equations are solved only for one-electron systems. A myriad collection of methods has been developed for approximating the solution for multiple electron systems so these approximations can be very helpful and valuable, but this needs some sophistication by a scientific researcher to know when each approximation is valid and how accurate the results are going to be **[10].**

4.AB INITIO METHODS AND THEIR PRINCIPLES

4.1 Ab initio methods

Ab initio methods are characterized by the introduction of an arbitrary basis for extend the molecular orbitals and then the explicit calculation all the required integrals that imply this basis. Ab initio calculations can be performed at the Hartree approximation level. Fock, which is equivalent to a calculation of the self-consistent field SCF (Self Consistent Field). The option and Hartree-Fock levels include correlation effects that are not included in the Hartree-Fock approximation level of a non-relativistic solution for the Hartree–Fock equation **[11].**

4.1.1 Hartree-Fock method

The orbital approximation describes the n-electron wave function as a product of n so-called spin orbital functions, associated with each electron. Schrödinger's equation at n electrons can be separated into n monoelectronic equations. However, the function of an n-electron wave described in this way does not satisfy Pauli's principle (the electrons are fermions), because it is not asymmetric under a permutation of two electrons. This problem is corrected when describing the wave function as a Slater determinant constructed from the n spin-orbitals (the n spin orbitals Ψ come from the n/2 space orbitals combined with two functions of spin α and β) **[12].**

The Hartree-Fock equation is solved by rewriting the spatial analysis of Molecular Orbitals in the form of a linear combination of Orbitals Atomic (OM=CLOA) giving rise to the Hartree-Fock-Roothaan (HFR) equations:

$$F\ C_k\ =\ e_k\ S\ C_k \qquad \textbf{(II-9)}$$

Where F is the Fock matrix, C_k is a column vector, and S is the matrix of collection.

The solution of the HFR equations is carried out in an iterative manner called Self Consistent Field (SCF) method.

4.1.2 Post HF methods

4.1.2.1 The electronic correlation

It is important to note that the Hartree-Fock theory does not take into account all of them

the correlation effects between electron motions within a system molecular. Thanks to the principle of antisymetry of the wave function, the electrons of same spin have zero probability

of occupying the same quantum box position. In in this case, the Slater determinant becomes equal to zero. On the other hand, nothing prohibits two electrons of different spins to occupy the same position at the same time! What results in an overestimation of energy with HF processing. This overestimation is Designated by correlation energy:

$$\mathbf{E_{corr=}\ E_{exact-}\ E_{HF} > 0}$$

Where E_{exact} is the exact energy of the system and E_{corr} is thus the missing energy associated with correlations in the exact many-body ground state wave function.$E_{exact}$is negative because$\mathbf{E_{HF}}$ is always the upper bound of the $\mathbf{E_{exact}}$.

4.1.2.2 Configuration Interaction (CI)

It is a single-reference method based on the variational approach. The Total wave function is a linear combination of several determinants each representing a possible configuration of electronic distribution. Sound principle: first, we establish according to the HF approach the Slater determinant of the fundamental wave function. Then, in this determinant several real orbitals are replaced by as many virtual orbitals. Finally, the total wave function, which is the linear combination of all these determinants, is obtained by minimizing the total energy of the system.

4.1.2.3 Møller-plesset (MPx)

These are methods based on the principle of perturbation. The system Hamiltonian is the sum of two contributions:

H0 which is the sum of the monoelectronic Fock operators and H' which is a small perturbation applied to H0. In the methods MPx (MP2, MP3...), electrons are excited (disturbed) at energy levels Virtual. The wave function obtained as a result of this excitation is calculated. The function of total wave would be the linear combination of all the configurations considered.

4.2 Principles of ab initio

Two equivalent formulations of QM were devised by Schrödinger and Heisenberg. Here, we will present only the Schrödinger form since it is the basis for nearly all computational chemistry methods **[10].**

- **The Schrödinger equation is:**

(II-11)

$$\hat{H}\,\Psi = \hat{E}\,\Psi$$

Where:

Ĥ represents the Hamiltonian of the system, accounting for the potential and kinetic energy of the system, while Ψ represents the wave function which contains all the information of the system. In a compact form H is given **[13]:**

$$H = T\,n + T\,e + V\,n\,e + V\,e\,e + V\,n\,n \qquad \textbf{(II-12)}$$

Where:

➢ **Tn** and **Te** are the kinetic energy operators for the nuclei and electrons,

➢ **Vne, Vee,** and Vnn are the potential energy operators for the nucleus-electron, electron-electron, and nucleus-nucleus interactions, respectively.

In atomic units H becomes:

$$H = -\frac{1}{2}\sum_{A}^{nuclei}\frac{1}{M_A/m_e}\nabla_A^2 - \frac{1}{2}\sum_{a}^{electrons}\nabla_a^2 - \sum_{A}^{nuclei}\sum_{a}^{electrons}\frac{Z_A}{r_{Aa}} + \sum_{A>B}^{nuclei}\sum_{B}^{nuclei}\frac{Z_A Z_B}{R_{AB}} + \sum_{a>b}^{electrons}\sum_{b}^{electrons}\frac{1}{r_{ab}} \qquad \textbf{(II-13)}$$

Where the Hamiltonian will include [**14]:**

➢ A: kinetic energy terms for the nuclei.

➢ a: Electrons.

➢ rAa: distance of separation (electron nucleus potential).

➢ RAB: distance of separation (nuclear-nuclear potential).

➢ rab: distance of separation (electron-electron repulsion).

Maybe it looks simply. But analytically, this equation is so hard to solve and impossible for more than two particles, and the problem is in the description of the correlated motion of many particles. So, to reach a solution, we must use a series of approximations. The first commonly used and one of the most conceptually important ones is the Born-Oppenheimer approximation **[15].**

- **Born-Oppenheimer approximation**

An approximation that can be made to realize that the motion of the nuclei is sluggish compared to the motion of the electrons due to the large differences in mass. So, because of the big difference in motion between the nuclei and the electrons, the electrons are capable of immediately adjusting to any change in the position of the nuclei. So, the electron motion is determined for a fixed position of the nuclei making the distances. RAB in Eq. (13) now a constant. This approximation is called the Born-Oppenheimer approximation.

The Born-Oppenheimer approximation removes the kinetic energy operators for the nuclear motion in Eq **(II.13).**

$$\hat{H} = -\frac{1}{2}\sum_{a}^{electrons} \nabla_a^2 - \sum_{A}^{nuclei}\sum_{a}^{electrons} \frac{Z_A}{r_{Aa}} + \sum_{A>B}^{nuclei}\sum_{B}^{nuclei} \frac{Z_A Z_B}{R_{AB}} + \sum_{a>b}^{electrons}\sum_{b}^{electrons} \frac{1}{r_{ab}} \quad \textbf{(II-14)}$$

The Schrödinger equation that is solved for then just becomes the electronic Schrödinger equation for the molecule more a constant term for the nuclear repulsion.

$$\hat{H}^{electronic}\,\Psi^{electronic} = \left(E^{electronic} + E^{nuclear}\right)\Psi^{electronic} \quad \textbf{(II-15)}$$

5. BASIS SETS AND FUNCTIONALS (DFT)

5.1 Basis sets

These are mathematical functions that describe orbitals atomic. There are several types of bases, you can use Slater type bases (STOs) or Gaussian type bases GTOs.

The Basics (STOs) allow to describe the electronic structure better than the GTOs bases.

that do not take into account the electrons closest to the nucleus and farthest away, but a Slater-type orbital can be obtained from a combination of Gaussian-type orbitals in which three Gaussian functions are combined to a Slater. In numerical calculations, orbitals of types are used a lot Gaussian because they reduce the drastic calculations of the electronic integrant. The smaller the chosen base, the poorer the representation of the wave function, the less precise the calculations.

5.1.1 The 6-31 G base

It is a base of the K-nlG type where K represents the number of Gaussians used to describe core electrons and – stands for split, i.e. treatment different from the valence orbitals and n+1 corresponds to the number of Gaussians used to describe valence electrons, we therefore have 6 Gaussian electrons to describe core electrons and 4 Gaussian electrons for valence electrons and G denotes a Gaussian.

5.1.2 The base $6-31\boldsymbol{G}^{*}$

Polarization functions are added to the 6-31G base. This allows you to better describe regions of space not described by the other functions. The links will be better described and the calculations will be more accurate.

5.1.3 The base 6-31G (+)

In this base a diffuse function is added to the 6-31G base, which allows to have a better representation of the molecular orbitals of the nucleus.

Example: The 6-31G base is very popular For a Carbon ($1S^{1}2S^{2}2P^{2}$):

- 6 Gaussians are used for the 1s core orbital.

- (-) stands for split-valence: the valence orbitals 2s and 2p are represented by orbital of core and valence.

- 3 Gaussians used to describe valence electrons, so we have 6 Gaussians to describe core electrons.

-1 Gaussian used to describe valence electrons.

If we add an asterix for the purpose of the notation (e.g. $6-31G^{*}$):

We add polarization terms, which will allow us to take into account the orbitals when the atoms approach each other. 2p orbitals are added to 2s orbitals in order to eliminate the isotropic character

spherical orbital of the 2s orbital, or we add 3D orbitals to the 2p orbitals to give asymmetric shapes, etc....

When we add 3d orbitals to the 2p orbitals of the atoms of the second line of the periodic table, we have a base denoted $6-31G^{*}$when we add 2p orbitals to the OA of the hydrogen atom, we have a base denoted $6-31G^{**}$[**A. L. Magalhães, 2014**][**16**].

5.2 Functionals

5.2.1 Exchange and correlation functionals

This exchange-correlation term is found at the level of the expression of the universal functional (universal means here that the functional is independent de $V_{ext}(\overrightarrow{r})$ for all systems) of Hohenberg and Kohn F_{HK}. We are therefore moving from an expression for which we do not know the mathematical form of the two functional $T_e[\rho]$ and $V_{ee}[\rho]$ Where the term E_{XC} represents what is not known, i.e., the exchange energy correlation through this approach, Kohn and Sham have transferred what is not known in the smallest term E_{XC}. As a result, the error made will be made on many small contributions to the total energy of the system. The exchange-correlation functional must take into account, in addition to the auto calculation, of the difference in kinetic energy between the non-interactive fictitious system and the real system. Thus, the calculation of energy and exchange-correlation potential is based on on a certain number of approximations which are the LDA and the GGA **[17].**

5.2.2 Approximation of local Density (LDA)

The first proposed in 1965 [3] by Kohn and Sham is that of density (LDA).

It consists in considering the correlation term as equivalent to that of a gas of homogeneous electrons. The term exchange and correlation are therefore separated into two:

$$E_{XC}^{LDA}[\rho] = E_X[\rho] + \int \rho(r)\ \varepsilon_C[\rho(r)]\, d^3r \qquad \textbf{(II-16)}$$

Where $E_{XC}^{LDA}[\rho]$ is the exact Fock exchange energy.

A slightly stronger approximation but with the advantage of coherence consists in considering the whole term of exchange and correlation as that of a homogeneous gas of electrons, hence:

$$E_{XC}^{LDA}[\rho] = \int \rho(r)\ \varepsilon_C[\rho(r)]\, d^3r \qquad \textbf{(II-17)}$$

Finding the function$[\rho(r)]$ is not trivial. This work is the subject of numerous studies that determine the values of what is called the exchange and correlation functional. The first precise evaluations were made in 1980 by D. Ceperley and B. J. Alder **[18],** and by Hedin Lindqvist (1972**) [19].** Other works such as J. P. Perdew and A. Zunger **[20]** or clarify, modify or slightly correct these values. But the results obtained by using one or the other functional are more or less equivalent.

5.2.3 Generalized Gradient Approximation (GGA)

A first step carried out with the aim of improving the treatment of the correlation exchange energy is to make the functional $E_{xc}[\rho(\vec{r})]$ dependent not only on the electron density but also on its gradient, $E_{xc}[\rho(\vec{r})]$. Thanks to this modification the functional $E_{xc}[\rho(\vec{r})]$accounts for the non-uniform nature of electron gas. In the formalism of the GGA, the contribution of $E_{xc}[\rho(\vec{r})]$ to the total energy of the system can be added cumulatively from each portion of the non-uniform gas as if it were locally non-uniform.

This definition of the GGA functional implies that it is of the form:

$$E_{xc}^{GGA}[\rho(\vec{r})] = \int \varepsilon_{xc}\,[\rho(\vec{r}), |\nabla\,\rho(\vec{r})|]\rho(\vec{r})\,\mathrm{d}\,\vec{r} \qquad \textbf{(II-18)}$$

In which $\varepsilon_{xc}\,[\rho(\vec{r}), \left|\nabla\overrightarrow{\rho(r)}\right|]$represents the exchange energy –electron correlation in a system of mutually interacting electrons of non-uniform density. The use of the GGA-type functional makes it possible to significantly increase the precision of the calculations compared to the description provided by the LDA, in particular for the binding energy of the molecules.

5.2.4 Choice of a functional

The choice of a functional depends on the system studied, its properties and the computation time. The functionals implemented in the Gaussian09 software **[21]** (B3LYP, PBEPBE, etc....) are hybrid functionals that do not require the computation of the Hartree Fock exchange term.

5.2.5 Hybrid functionals

In these functionals, a certain percentage of the exact exchange is introduced computable as in HF theory. Becke proposed the following expression of energy exchange and correlation, qualified as hybrid because it takes into account energy HF as well as the exchange and correlation energy DFT **[22].**

$$E_{hybride}^{XC} = C_{HF}E_{HF}^{X} + C_{DFT}E_{DFT}^{XC} \qquad \textbf{(II-19)}$$

The parameters C_{HF} and C_{DFT} being constants to be determined. The most popular functional hybrid is known as the B3LYP. It is proposed by Becke as an expression of three parameters designated by B3 **[23]** and uses the B88 approximation for the exchange and the Lee, Yang and Parr (LYP) approximation for the correlation. It allows to correctly describe the magnetic properties of organic molecular compounds and also of transition metals and ligands **[24,25**]. In turn, these functionals treat the exchange part of the functional as a mixture of Hartree-Fock exchange and DFT exchange. The correlation part remains purely DFT. They allow for a

better energetic representation of the exchange-correlation energy. The best functional ones at the moment are hybrid functionals.

6. MOLECULAR GEOMETRY OPTIMAZATION

Geometry optimization seeks the nearest local energy minimum or transition state. This means that the resulting structure is dependent on the starting geometry. Different initial geometries may lead to different optimized structures.

The chosen quantum mechanical method and basis set play significant roles in the accuracy and reliability of the optimized geometry.

While the goal is to find the global minimum (the absolute lowest energy structure), in practice, geometrical optimization often finds local minima. Additional techniques may be needed to ensure that the global minimum has been located **[26].**

7. ENERGY MINIMIZATION TECHNIQUES

7.1 Introduction

Minimization sometimes results in hydrogens and doublets arranged around the atom in impossible structural positions. This is often due to movement inappropriate initial exposure of these light atoms when a strongly distorted structure is introduced. This can also happen if you start with a planar structure. This is why the program performs a minimization "second pass" after repositioning the atoms Light. Another difficulty of minimization concerns the problem of the local minimum. The constraint optimization routines, have the unfortunate tendency to find the minimum energy closest to the input structure. In general, the distances and connecting angles are properly minimized, so well that the problem of the local minimum can be summed up in the optimization of dihedral angles (it is necessary to much more energy to deform a bond or valence angle relative to a dihedral angle). The following approaches aim to extract the molecule from its potential **[27].**

Almost all minimization methods have at least one thing in common:

starts at a given point in the hypersurface and descends to the lowest minimum close, without knowing whether this minimum is local or absolute.

Minimization algorithms for a molecule with N atoms, the function to be minimized therefore includes 3N Variables. Such a function generally includes an overall minimum and

minimizations. premises. From the initial geometry, we look for the set of Cartesian coordinates that minimizes the sum of all energy contributions. In principle, it is sufficient to take the first derivative of steric energy with respect to each of the degrees of freedom of the molecule and find the place on the hypersurface where, for each coordinate ri, (dE/dri) = 0. The procedures for achieving this goal are of two types:

the slope of the surface (first derivative), the others, both this slope and the curvature of the surface (the first and second derivatives).

7.2 The steepest descent method

The first minimization program that can perform a geometry is due to Wiberg **[28]** and uses the steepest descent method. After calculating the energy corresponding to an initial geometry, each atom is moved individually according to its three Cartesian coordinates and the energy is recalculated after each displacement.

7.3 The conjugate gradient method

This method, based on the same principle as the previous one (opposite direction to the energy gradient), also takes into account the previous steps, in order to determine more finely the direction and the step. For a quadratic energy surface, a function of 3N variables, this method converges in 3N pas **[29].**

7.4 The Newton-Raphson method

A further improvement in convergence can be achieved by having use of a quadratic approximation Q of the function F, obtained by expanding in Taylor's series **[30].**

The method consists in seeking at each step the minimum of development to order 2 of function F. This method, known as the "Newton-Raphson" method, uses derivatives Seconds. Now we use this optimization technique instead. It evaluates the second derivatives of molecular energy with respect to geometric parameters and is therefore converging more quickly.

7.5 The simulated annealing method

The methods we have just described have the particularity of reducing each step the function F; These methods cannot therefore escape the local minimum close to the initial structure, and consequently have a radius of convergence always restricted. The simulated annealing method

"ring", developed by Kirkpatrick **[31],** allows the function F to be increased momentarily in order to cross energy barriers to fall back in a deeper minimum.

8. CALCULATION OF VIBRATIONAL PROPERTIES

8.1 Vibrational analyses of the molecule

Molecular modeling also allows the study of the motions of atoms in the molecule. Infrared (IR) absorption spectrometry was used for the study of the modes of the vibration of our molecule. They are based on the principle of matter-radiation interaction.

8.2 General concept

Infrared absorption spectroscopy is a structural analysis technique based on vibrational analysis of bonds **[32];** it is useful for determining the types of bonds (functional groups) present in a molecule. The infrared range extends from 0.8µm to 1000µm. It is divided into 3 categories, the near-infrared (0.8 to 2.5 µm or 14000-4000 cm^{-1}), mid-infrared (2.5 to 25 µm or 4000-400 cm^{-1}) and the far infrared (25 to 1000 µm or 400-200 cm^{-1}).

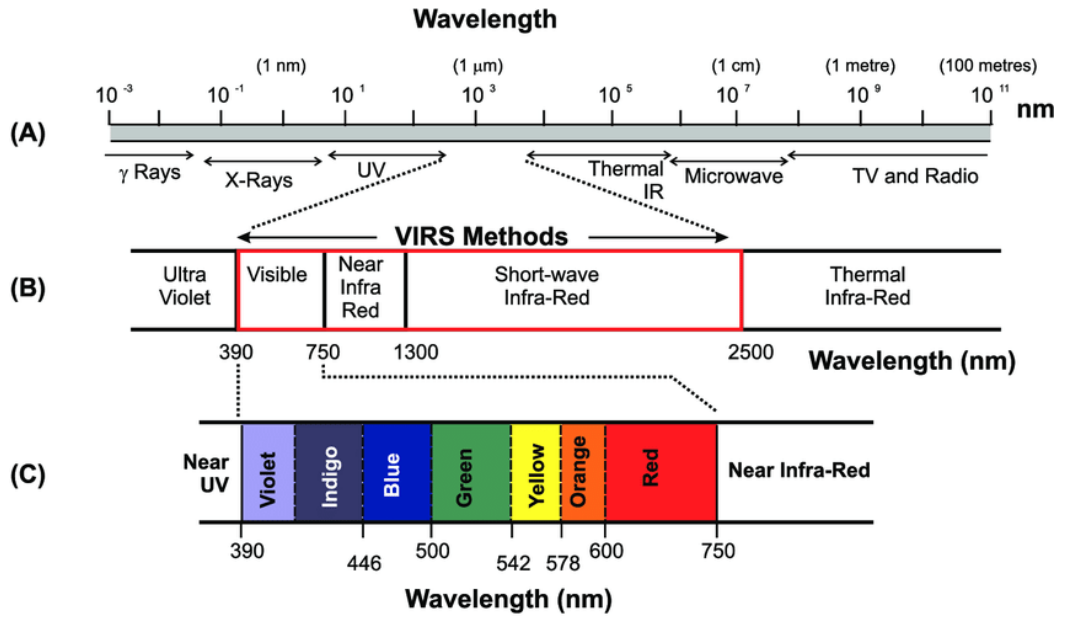

Figure II-9: The electromagnetic spectrum

[**Source : Ali Abdulridha Al Maliki,2015**. *https://www.researchgate.net/figure/Portions-of-the-electromagnetic-spectrum-highlighting-the-regions-of-interest-for_fig1*_313505689]

8.3 Molecular vibration modes

A molecular vibration occurs when the atoms of a molecule are in a periodic motion while the molecule as a whole undergoes a periodic motion of translation and rotation. The frequency of the periodic motion is called the frequency of vibration. A vibration is an oscillatory movement, so we can model the molecule as a set of oscillators linked to each other. All the atoms of the molecule, vibrate with a frequency around their equilibrium position. Each of these vibrations is called normal mode of vibration. We know that a nonlinear molecule has N atoms, it therefore has 3N degrees of freedom, 3 corresponds to the translation of the molecule and 3 to its rotation around its center of inertia. There are therefore 3N-6 normal modes of vibration, i.e. 3N-6 possible vibration frequencies (at maximum), whereas a linear molecule has none than 3N-5, since rotation around its molecular axis cannot be observed **[33,34]**. Simple vibrations can be classified into two main groups: stretching and bending.

8.3.1 Elongation vibrations (stretching) or valence vibrations

A valence vibration (elongation or elongation) is a movement of the atoms along the axis of the bond. This movement implies a variation in distance interatomique. They are two types:

- Symmetric vibration with conservation of molecular symmetry.
- Asymmetrical vibration with loss of one or more elements of symmetry of the molecule that requires more energy.

8.3.2 Vibration bending

Strain vibrations have lower intensities than valency. These vibrations correspond to a change in the angles of the bonds and constitute the region of the spectrum known as the "fingerprint" (1000 cm^{-1} to 600 cm^{-1})

8.4 Classification of vibration modes

Vibrations can be classified into two categories: in-plane and out-of-plane **[35,36]**as in Figure10.

- In the plane: a distinction is made between symmetrical and antisymmetric angular deformations correspond to the shearing (scissoring) or rotational (rocking) movements of three atoms forming the angle.

- Out of the plane: these are the angular deformations outside a molecular plane that can induce a collective movement of the molecule corresponding to twisting (τ) or wagging (γ) movements.

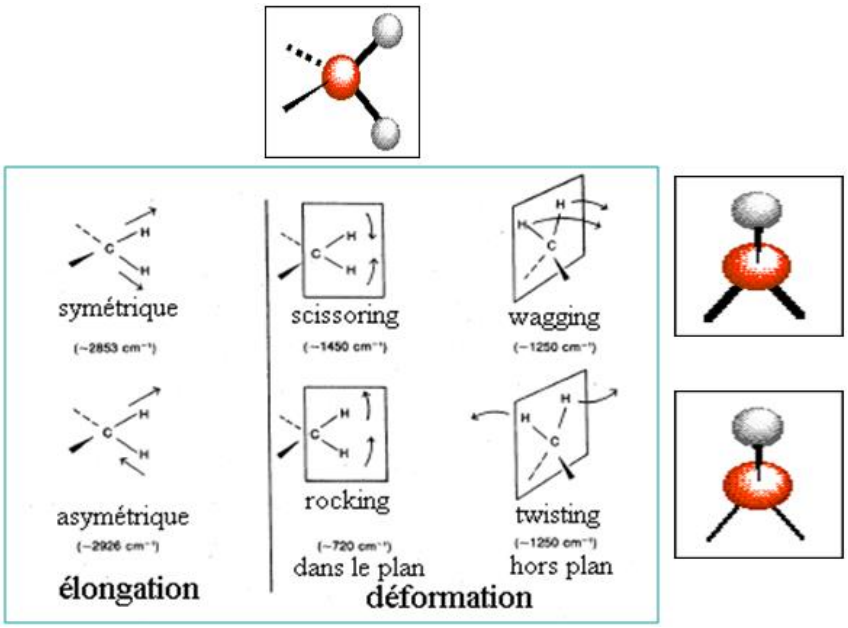

Figure II-10: Mode vibration of molecular

[**Source** ***:****https://chimieanalytique.com/spectroscopie-moleculaire-infra-rouge/.**2025***]

A movement of vibration is a movement internal to the molecule:

variation of interatomic distance, of bond angle, for a diatomic molecule A-B, the only internal vibration movement is the variation of the distance rAB. In a Vibration movement is a movement internal to the molecule: variation of molecules poly atomic, the situation is more complex. The bonds undergo movements of angular deformation that modify the angulations between bonds.

It can be shown that for a polyatomic molecule of n atoms, there exists:

- (3n-6) vibrational motion if the molecule is nonlinear
- (3n-5) Vibrational motion if the molecule is linear

These movements of vibration are called normal modes of vibration. A mode normal vibration is a synchronous vibration movement of atoms or groups atoms that can be excited independently of other normal modes of vibration of the molecule The vibrational energy is given by the following equation:

$$\sum_{i=1}^{N-6} E\,v = \sum_{i=1}^{3N} hwi\,(vl + \frac{1}{2}) \qquad \textbf{(II-20)}$$

8.4.1 Vibration frequency

If we have both masses mA and mB at the equilibrium distance r0, the latter begins to oscillate.

The oscillation frequency is given by Hooke's law.

$$V = \frac{1}{2\pi}\sqrt{\frac{K}{\mu}} \qquad \textbf{(II-21)}$$

$$\mu = \frac{mA\ mB}{mA + mB} \qquad \textbf{(II-22)}$$

With vibration frequency

μ: reduced mass

K: bond strength constant

mA et mB: mass of atoms A and B respectively

By convention: units in vibrational spectroscopy are wavenumbers: [cm−1]

The frequency or number of vibration waves of the A-B system depends on μ and k.

8.4.2 Vibration energy

To describe the forces acting on a vibrating bond, energy is used potential of a harmonic oscillator given by:

$$EP = \frac{1}{2}KX^2 = \frac{1}{2}K(r - r0)^2 \qquad \textbf{(II-23)}$$

In the case of the harmonic approximation, the Schrödinger equation as a function of direction is

$$-\frac{h^2}{2\mu}\frac{d^2}{dx^2}\Psi(X) + \frac{1}{2}KX^2\Psi(X) = E\Psi(X) \qquad \textbf{(II-24)}$$

And its solution is:

$$Ev = h\left(\nu + \frac{1}{2}\right) \qquad \textbf{(II-25)}$$

V: quantum number of vibration (0, 1,2...).

ν: vibration frequency determined in the classical model.

References Bibliography

[1] **R. Ursula** *Introduction to Electronic Structure Methods. EPFL, Lausanne, 2017.*

[2] **Y. Tua, A. Laaksonen.** *Advances in quantum chemistry Chapter 1 - Implementing Quantum Mechanics into Molecular Mechanics—Combined QM/MM Modeling Methods. 2010, 59, 1-15.*

[3] **A: Parr. R. G. and Yang. W**. *« Density Functional Theory », Oxford University Press, (1989).*

B: Bartolotti. L. J. and Flurchick. K., Rev. *Comput. Chem., 7, (1996), 187*.

[4] **Hohenberg. P. and Kohn. W**., Phys. Rev**.,** *136, (1964), B846***.**

[5] **P. Hohenberg, W. Kohn**, Phys. Rev. B *136, 864 (1964)***.**

[6] **D. Laxmi and S. Priyadarshy,** *'HyperChem 6.03', Biotech Softw. Internet Rep. Comput. Softw. J. Sci., vol. 3, no. 1, pp. 5–9, 2002.*

[7] **M. Caricato, M. J. Frisch, J. Hiscocks, and M. J. Frisch,** *Gaussian 09: IOps Reference. Gaussian, 2009.*

[8] **'software-index'.** *Accessed: Jun. 08, 2023. [Online]. Available: https://sites.google.com/view/molecvue/software-index*

[9] **A. Shandilya, S. Chacko, B. Jayaram, et I. Ghosh**, *« A plausible mechanism for the antimalarial activity of artemisinin: A computational approach », Sci. Rep., vol. 3, n^o 1, p. 2513, août 2013, doi: 10.1038/srep02513.*

[10] **David C. Young.** *Computational Chemistry: A Practical Guide for Applying Techniques to Real-World Problems, 2001, 10-44.*

[11] **W.C. Ripka & J.M. Blaney**, *''Topics in Stereochemistry", Eds. Eliel & Wilen, 1991*

[12] **N. Vulliermet,** *Thèse de doctorat, Université de Genève (Suisse), 2000.*

[13] **M. Izquierdo, A. Maria.** *Large Scale Modelling of Photo-Excitation Processes in Materials with Application in Organic Photovoltaics. [Groningen]: University of Groningen, 2019.*

[14] **M.A. Michael.** *Molecular Spectroscopy and Modern Electronic Structure Computations, Rose-Hullman Institute of Technology Terre Haute, Indiana. 2001, 222-235.*

[15] **G. D. Mickael.** *Extending the Reach of Accurate Wavefunction Methods. Digital Comprehensive Summaries of Uppsala Dissertations from the Faculty of Science and Technology 1228. Uppsala: ActaUniversitatisUpsaliensis, 2014.*

References Bibliography

[16] **A. L. Magalhães,** *« Gaussian-Type Orbitals versus Slater-Type Orbitals: A Comparison », J. Chem. Educ., vol. 91, n° 12, p. 2124-2127, déc. 2014, doi: 10.1021/ed500437a.*

[17] **A. ROUABHIA,** *Thèse de Magister " Étude ab initio des propriétés structurales et Magnétiques des antipérovskites Fe3MC (M= Zn, Al, Ga, et Sn)". Université des Sciences et de la Technologie d'Oran- Mohamed Boudiaf, (2010).*

[18] **D.M. Ceperley and B.J. Alder***: Ground state of the electron gas by a stochastic method. Physical Review Letters, 45(7):566, 1980***.**

[19] **L. Hedin and B. I. Lundqvist. J. Phys***. C4, 2064 (1980).*

[20] **J.P. PERDEW and A. ZUNGER:** *Self-interaction correction to density-functional Approximation for many-electron systems. Physical Review B, 23(10):5048, 1981.*

[21] **M. J. Frisch, G. W. Trucks, H. B. Schlegel, G. E. Scuseria,** *Gaussian, Inc., Pittsburgh PA, 2003.*

[22] **Boucekkine, G.** *méthodes de la chimie quantique, Edition TI, AF6050 2007***.**

[23] **Becke, A. D. 1.** *Chem. Phys. 1993,98,5648-5652.*

[24] **Lee, C.; Yang, W.; Parr, R. G.** *Physical review B 1988, 37, 785*

[25] **Lee, c.; Yang, W.; Parr, R G.** *Phys. Rev. B 1988, 37, 785***.**

[26] **«** *Part 3 - Introduction to Geometrical Optimizations », atomistica. Online. Consulté le : 11 mars 2025. [En ligne]. Disponible sur : https://atomistica.online/course-what-is-molecular-modeling/part-3-introduction-to-geometrical-optimizations/*

[27] **V. Brenner, thèse de doctorat, Université de Paris-Sud, octobre,** *1993*

[28] **K.B. Wiberg, J.Am. chem. Soc. 1965, 87,1070.**

[29] **W.H. Press, B.P. Flanning, S.A. Teukolsky et W.T. Vetterling,***"Numerical Recipies", Cambridge U.P., New-York, pp.274, 1986.*

[30] **A. Warshel and S. Lifson,** *J. Chem.Phys,1970, 53, 582.*

[31] **S. Kirkpatrick, C.D. Gellet, M.P. Vecchi***, Science,1983, 220,671.*

References Bibliography

[32] Slater, J.C. *Pysi. Rev, 36, 57, 1929.*

[33] Berthier G., *Chem J. Phys. 51, 363, 1954.*

[34] Pople J. A. et Nesbet R. K., *J. Chem. Phys. 22, 571, 1954.*

[35] Hinchcliff A., 'Modeling Molecular Structure', Wiley & Sons, *Chester 1996.*

[36] Slater J. C., *Phys. Rev. 57, 57, 193*

Part II: Experimental

CHAPTER III: METHODOLOGY

Part II: Experimental

Chapter III: Methodology

1. Introduction

To investigate the structural and electronic properties of the artemisinin and glucose molecules, a computational chemistry-based approach was adopted in this study. Specifically, this method relies on **density functional theory (DFT)**, which enables accurate simulation of molecular systems while maintaining a reasonable computational cost.

Determining the optimal geometry of artemisinin and glucose, analyzing its vibrational modes, and appreciating its electronic properties, such as boundary orbitals (HOMO-LUMO), as well as its spectroscopic suitability through IR modeling are the primary goals of this study.

This has been accomplished by using a number of specialist programs:

- Gauss View 6.0 is used to visualize and elaborate molecular structures.
- Gaussian 09 for quantum computations (DFT, vibration analysis, optimization),

The approach adopted in this work is explained in detail in the later parts, covering from the elaboration of the structures to the analysis of the theoretical results obtained.

2. Molecular structure

✓ Artemisinin, a sesquiterpene lactone with the molecular formula $C_{15}H_{22}O_5$, was extracted from *Artemisia*. Its molecular weight is 282,14 (g/mol), and chemical and spectroscopic investigations have established its structure.

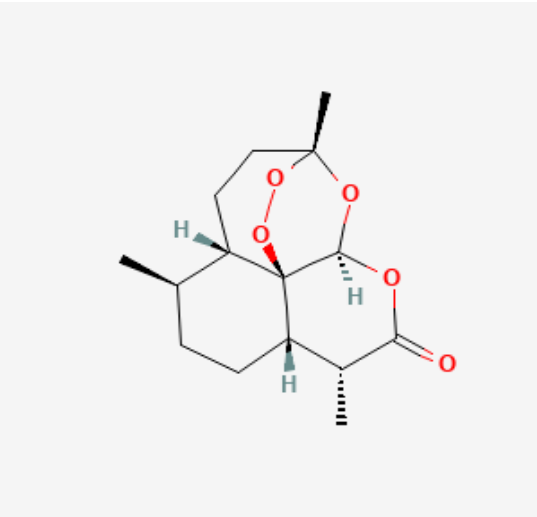

- ✓ Glucose is a monosaccharide belonging to the osesfamily, specifically, it is an aldohexose, which is a sugar with six carbon atoms and an aldehyde group, molecular weight is 180,16 g/mol, its basic chemical formula is $C_6H_{12}O_6$.

[Source : pubchem, 2021. *https://pubchem.ncbi.nlm.nih.gov/]*

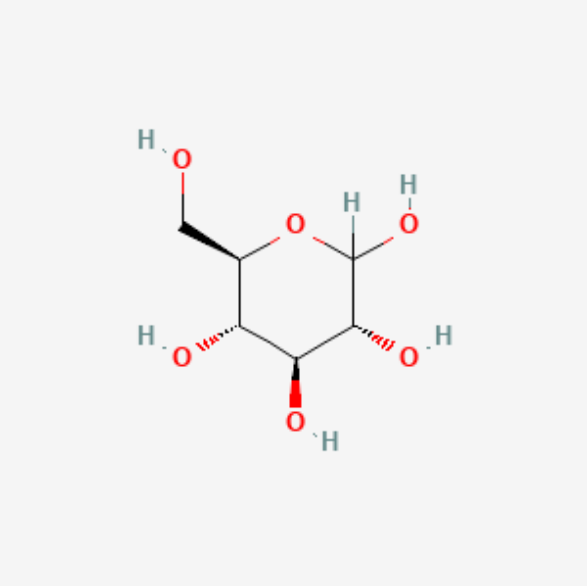

Figure III-12: Molecule of glucose (2D)

[**Source : ChEBI,2025**. *https://www.ebi.ac.uk/chebi/searchId.do?chebiId=CHEBI:4167]*

3. Molecular geometry and input preparation

- ✓ Artemisinin displays intricate geometric elements of sesquiterpene lactones in three dimensions (3D). The structure is made up of a 1,2,4-trioxane endoperoxide bridge and a fused tricyclic backbone.

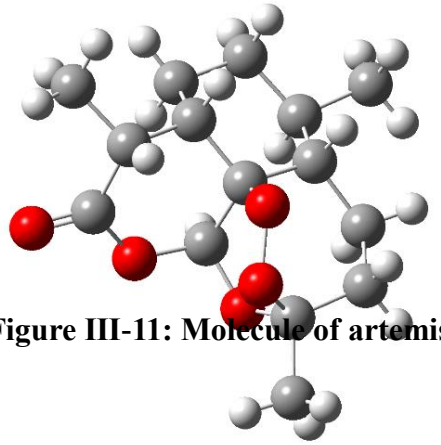

Figure III-11: Molecule of artemisinin(2D)

The molecule is composed of five oxygen atoms, twenty-two hydrogen atoms, and fifteen carbon atoms ($C_{15}H_{22}O_5$). Artemisinin has a distinct chirality because of its many chiral centers.

- ✓ As is typical of aldohexoses, glucose has a comparatively straightforward but extremely important three-dimensional (3D) structure. 6 carbon atoms, 12 hydrogen atoms, and 6 oxygen atoms make up the molecule ($C_6H_{12}O_6$).

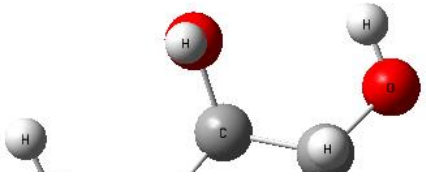

Figure III-14: Molecule glucose (3D)

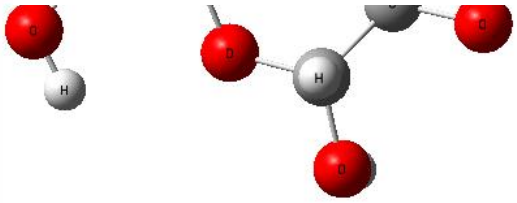

It has several chiral centers, which provide distinct stereochemistry and allow for the existence of several structural isomers.

The input file was prepared with the following specifications:

- **Method:** B3LYP
- **Basis set:** 6-31G++ (d', P')
- **Job type:** Geometry optimization followed by vibrational frequency analysis
- **Charge:** 0 (neutral molecule)
- **Multiplicity:** ground state

Figure III-13: molecule of artemisinin (3D)

4. Computational tools and software

The artemisinin molecule was modeled and analyzed using computational tools and software as part of this effort.

- ❖ The primary software utilized was as follows:

Gaussian 09 is a quantum computation program that is used for density functional theory (DFT) and ab initio calculations.

Gaussian software Gaussview 6.0 enables the creation and manipulation of molecular structures (such as glucose and artemisinin) in three dimensions.

5. Software packages (gaussian and gaussview)

This experiment was completed by building, modeling, calculating, and analyzing the properties of the glucose and artemisinin molecules using software designed specifically for computational chemistry.
Gaussian 09 in this work it was used to:

- Optimize the geometry of the artemisinin and glucose molecules,
- Calculate vibrational frequencies,
- Determine the electronic properties (total energy, HOMO-LUMO),
- Simulate the infrared spectrum

The calculations were made with the basis set B3LYP/6-31G++ (d', P'), to have a precision on the results.

GaussView 6.0 in this work It was used to:

- Construct the initial geometry of the molecule,
- Prepare input files for calculations,
- Visualize optimized structures,
- molecular orbitals, and vibrations.

Gaussview makes it easy to set up calculations and interpret results.

6. Geometry optimization

A geometric optimization of the glucose and artemisinin molecules was carried out in order to identify the most energetically stable configuration. This phase is crucial before moving on to

more accurate computations like vibrational frequencies or electronic transitions. GaussView 6.0 was used to do the initial constitution of artemisinin and glucose while maintaining the proper stereochemistry of the molecules.

7. Methods used for optimization (DFT)

Next, we used the Gaussian software to optimize the geometry integrally at the B3LYP/6-31G++ (d', P') level using density functional theory (DFT). When examining organic compounds, this method is known to offer a good balance between computing cost and accuracy.

The calculations were carried out in the gas phase, with the following parameters:

- **Method:** B3LYP
- **Basis set:** 6-31G++ (d', P')
- **Total charge**: 0 (neutral molecule)
- **Spin Multiplicity**: Default spin
- **Convergence criteria**: default (according to Gaussian 09standards)
- **Job type:** optimization
- **Multiplicity:** ground state

8. Vibrational analysis

Following geometry refinement, a vibration analysis was performed to verify that the final structure accurately depicts a minimum of energy on the potential surface. Predicting the molecule's typical vibration modes and their precise frequencies is another benefit of this phase.

The Gaussian software was used to execute the calculations in a gas and water phase at a theoretical level that was the same as the geometric optimization (B3LYP/6-31G++ (d', P')).

The examination of the vibration frequencies led to the obtaining of:

- The set of frequency values expressed in cm^{-1},
- The intensities associated with each mode (IR),
- Atomic displacement vectors,
- viewable in animated form via GaussView 6.0.

❖ **Validation criterion:**

The optimal structure corresponds to a local minimum on the potential energy surface rather than a saddle point or transition state, as seen by the absence of imaginary frequency (negative values).

9. Calculation of other physico-chemical properties

A number of physicochemical properties (HUMO-LUMO gap energy, ionization energy, electron affinity, electronegativity, chemical hardness, and electrophilicity) were computed using quantum chemistry techniques, specifically using Gaussian 09software and visualization through GaussView 6.0, in order to gain a better understanding of the electronic and reactive properties of the artemisinin and glucose molecules.

CONCLUSION

A well-planned methodology was used in this artemisinin and glucose investigation to accomplish a number of goals, such as figuring out the material's ideal shape, assessing its vibrational modes, and looking into its electrical and spectroscopic characteristics. In this case, Gaussian09 was used for quantum chemistry computations, and GaussView 6.0 was used for result display and interpretation. This approach made it easier to simulate the infrared spectrum, optimize molecular structure, and assess crucial factors including chemical hardness, electronegativity, and HOMO-LUMO energies, as well as electrophilicity. Thus, this scientific approach offers a strong basis for a thorough comprehension of the structural and reactive properties of glucose and artemisinin.

CHAPTER IV: RESULTS AND DISCUSSION

Chapter IV: Results and discussion

1. Introduction

In this part, we present and study the computational results from quantum chemistry calculations performed on the molecule studied. The discussion begins with optimized molecular geometry, which offers a perspective on the stable conformation of the system. We analyze structural parameters such as bond lengths, bond angles, and dihedral angles to evaluate geometric features and their compliance with usual chemical expectations or available experimental data.

Subsequently, the vibrational properties are examined to validate the stability of the optimized structure (i.e., the absence of imaginary frequencies) and to interpret the characteristic vibrational modes that can be attributed to specific functional groups present in the molecule.

We then address the electronic properties with an emphasis on the energies of the molecular boundary orbitals (HOMO and LUMO). The energy gap between HOMO and LUMO is a key indicator of the chemical reactivity and kinetic stability of the molecule, providing valuable information about possible electronic transitions and charge transfer capabilities.

Ultimately, structure-property relationship analysis explores the correlation between the computed molecular structure and its predictive properties. This integrated approach provides an in-depth understanding of the molecule's behavior and reactivity, guiding future functional or application-oriented studies.

Part I: Results and discussion of artemisinin

2. Optimized molecular geometry

The DFT/B3LYP/6-31G++ (d', p') method was used for the geometric optimization of artemisinin in two different environments: in the gas phase and in the aqueous phase.

ΔE = E(water) – E(gas) = kcal/mol **(IV-26)**

1Hatree (Ha) = 27.2114 eV

1eV =23,06 kcal/mol

File type	.chk
Calculation type	Final OPT
Calculation method	RB3LYP
Basis set	6-31G++ (d', P')
Charge	0
Spin	Singlet
Solvation	None
Electronic Energy	-26062,05873 eV
RMS Gradient Norm	583,8748679 $eV/Bohr$
Dipole moment	6,0969737 Debye
Imaginary freq	

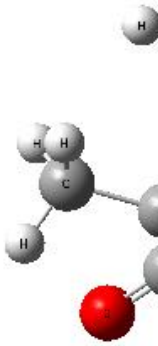

Figure IV-16: Artemisinin optimization in the gas phase

Table 1-IV: Summary in gas phase

File type	.chk
Calculation type	Final OPT
Calculation method	RB3LYP
Basis set	6-31G++ (d', P')
Charge	0
Spin	Singlet
Solvation	Srcf=solvent=water
Electronic Energy	-26148,96689 Ev
RMS Gradient Norm	5,17× 10^{-4} $eV/Bohr$
Dipole moment	8,551771 Debye

Figure IV -15: Artemisinin optimization in the aqueous phase

Imaginary freq	

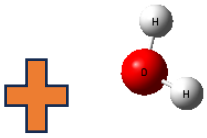

Table 2-IV: Summary in aqueous phase

ΔE = (-26148,96689 +26062,05873)× 23,06= -2003,476252kcal/mol

ΔE < 0 the molecule is more stable in the aqueous phase.

The fact that there are no imaginary frequency attests that the structure is a global minimum, Artemisinin shows notable differences in terms of conformation and energy when it is geometrically optimized in gas and in an aqueous solution. These results highlight the crucial role of the environment in research on stability and biological activity.

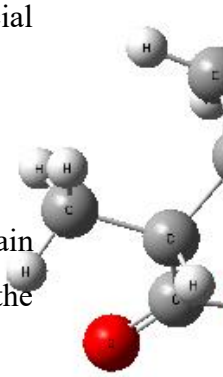

3. Bond lengths, bond angles, and dihedral angles

We extracted and compared the bond lengths, valence angles and dihedral angles of the main functional groupings. The observed geometric variations allow us to assess the effect of the solvent on the molecular structure.

a) Bond lengths

Table 2-IV: Summary in aqueous phase

Functional group	**Gas (Angstrom)**	**Water (Angstrom)**	**Experimental**	**Variation**
$O_1 - O_2$ (Peroxide)	1,469 A°	1,459 A°	1,469 A°	-0,01 A°

$O_2 - C_{11}$ (Lactone)	1,462 A°	1,464 A°	1,416 A°	+0,002 A°
$C_{11} - C_{12}$ (Pont epoxy)	1,522 A°	1,540 A°	1,53 A°	+0.018 A°

Table 3-IV: Bond lengths

A slight narrowing of the O-O bond in aqueous medium is noticed, suggesting a potential increase in local polarity caused by the solvophilic environment.

b) Bond angles

Functional group	Gas	Water	Experimental	Variation
$O_2 - 0_1 - C_9$(Peroxide)	108,098°	108,941°	108,100°	+0,843 °
$O_2 - C_{11} - C_6$ (Epoxide)	106,284°	106,300°	106,600°	+0,016 °
$C_6 - C_{11} - C_{12}$ (Lactone)	113,453°	112,871°	114,200°	-0,582 °

Table 4-IV: Bond angles

These modifications, although slight, reflect a local reorganization of the geometry favored by the interaction with the solvent, in particular around the oxygen functions.

c) Dihedral angles

Functional group	Gas	Water	Experimental	Variation
$O_2 - O_1 - C_9 - O_3$	−75,537°	-73,876°	-75,500 °	+1,494 °
$C_{10} - O_3 - C_9 - O_1$	35,001°	35,115°	36,000 °	+0,114 °

Table 5-IV: Dihedral angles

The dihedral angle around the peroxide group reveals a subtle rotation in solution, which can affect chemical reactivity.

The comparative study of the geometric characteristics in gaseous medium and in aqueous solution reveals that the solvent has a slight effect on the structure of artemisinin, particularly around the peroxide bond and the oxygen rings.

4. Vibrational properties

A frequency analysis (vibration measurement) was performed to confirm the nature of the run-up.

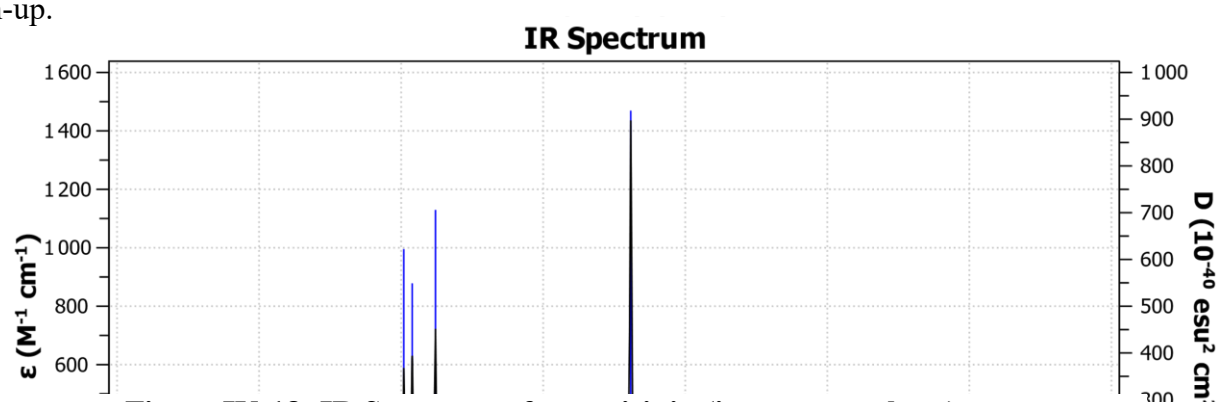

Figure IV-18: IR Spectrum of artemisinin (in aqueous phase)

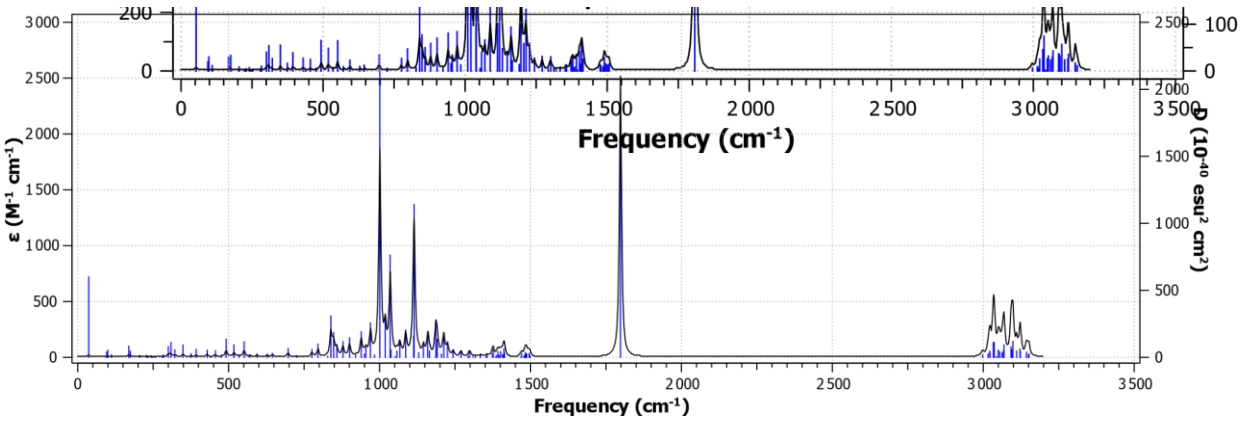

Figure IV-17: IR Spectrum of artemisinin (in gas phase)

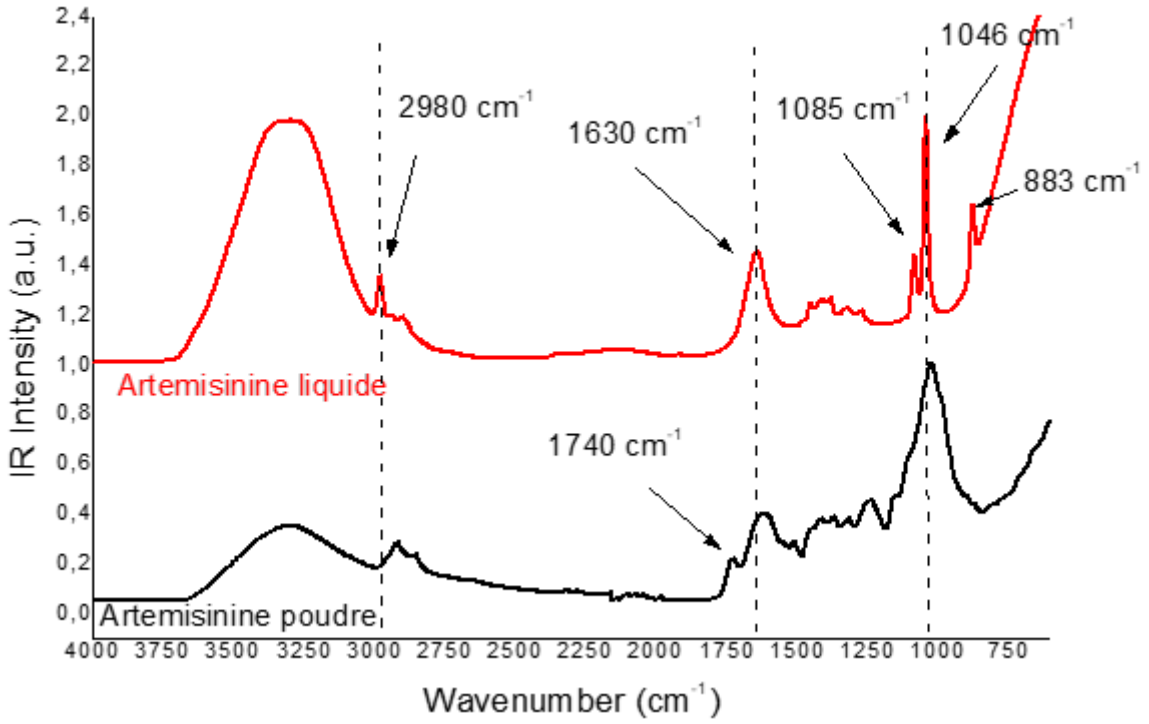

Figure IV-19: Experimental IR Spectrum of artemisinin

Functional group	**Mode of vibration**	**Band characteristic (gas) cm^{-1}**	**Band characteristic (water) cm^{-1}**	**Experimental**
1-lactone group (keto-lactone cycle) $C = O_5$	Elongation	~1808,17	~1798,32	1740
2-endoperoxide cycle ($O_1 - O_2$)	Elongation	~858,93	~828,16	883
3-methylene and methyl groups (C-H)	CH_3 { Scissoring, Rocking, Wagging, Twisting }	{ ~1417,57 – 1477,76, ~1009,98 – 1120,58, ~1372,87 – 1359,81, ~1148,26 }	{ ~1401,74 – 1410,25, ~954,57 – 983,10, ~1317,71 – 1356,35, ~1243,56 – 1269,62 }	

	CH_2 {Scissoring, Rocking, Wagging, Twisting}	{~1406,24, ~725,98, ~1352,42, ~1148,26}	{~1393,06 – 1396,32, ~697,12, ~1317,71, ~121,57}	~1250-1500
4- C-O bonds (ester, ether) lactone and ether cycle (C-O_4 – C)	Elongation	~1009,38-1020,13	~1009,92	1046
5- tetrahydrofuran cycle (THF) furan cycle (C-O_4 – C))	Elongation	~1113,95	~1145,08	1085

Table 6-IV: Interpretation of the IR Spectrum of artemisinin

These spectroscopic variations verify that the aquatic environment has a measurably structural and vibrational influence on artemisinin, primarily at the level of functional oxygen groups. This may have an effect on the protein's biological activity and molecular interactions.

5. Electronic properties

Electrostatic potential analysis makes it possible to identify preferred sites of attack for either a nucleophile or an electrophile by highlighting areas that are rich or poor in electrons.

- Blue: Represents areas of high positive potential, located near electron acceptor sites.
- Red: Indicates The area of high negative potential is associated with a high electron density.

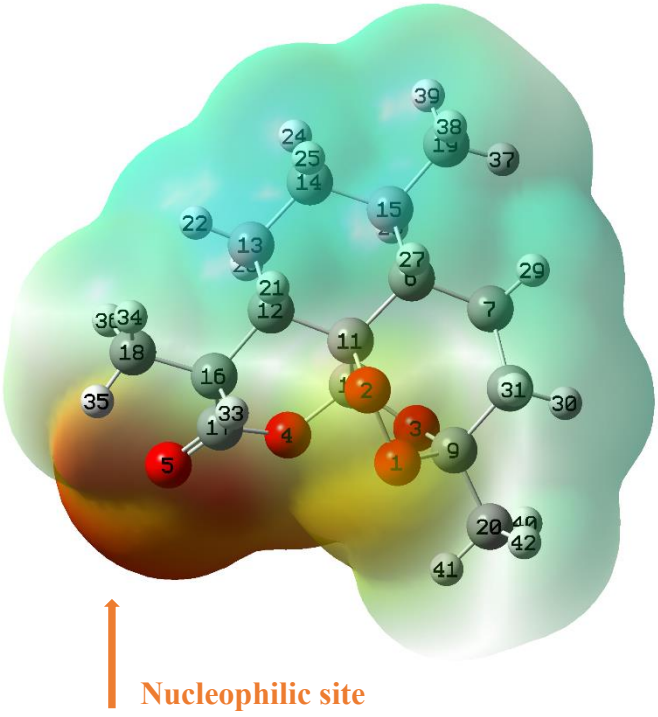

Figure IV-20: Electrostatic Potential (ESP) of artemisinin

❖ According to Koopmans theorem, in the framework of the Hartree-Fock closed-shell (HF) theory, the energy of first ionization of a molecular system corresponds to the inverse of the orbital energy of the highest occupied molecular orbital (HOMO).

parameter	**Artemisinin (Gas eV)**	**Artemisinin (water eV)**
Energy of the gap $E_{gap} = E_{LUMO} - E_{HUMO}$	*6,83*	*6,85*
Ionization Energy $E_i = -E_{HUMO}$	*7,33*	*7,44*
Electron Affinity $E_A = -E_{LUMO}$	*0,50*	*0,59*
Electronegativity $\chi = -\frac{(E_{HOMO} + E_{LUMO})}{2}$	*3,91*	*4,01*
Chemical Potential $\mu = \frac{(E_{HOMO} + E_{LUMO})}{2}$	-3,91	-4,01
Chemical Hardness $\eta = \frac{(E_{HOMO} - E_{LUMO})}{2}$	-3,41	-3,42
Chemical Softness $S = \frac{1}{\eta}$	-0,29	-0,30
Electrophilicity Index $\omega = \frac{\mu^2}{2\eta}$	2,24	2,35

Nucleophilicity Index $\varepsilon = \frac{1}{\omega}$	0,44	0,43

Table 7-IV: Global parameter (artemisinin)

Although it displays electrical polarization, artemisinin is generally stable. The electrophilicity index and electron affinity both rise when a water-based solvent is present, indicating a stronger electrophilic nature and improved electron acceptance in biological environment**.**

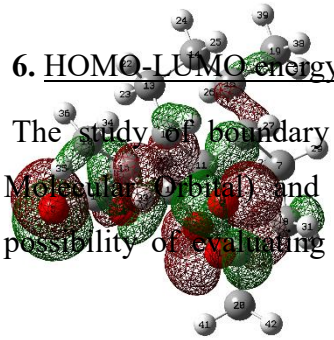

6. HOMO-LUMO energy gap and implications for reactivity

The study of boundary molecular orbitals, in particular the HOMO (Highest Occupied Molecular Orbital) and the LUMO (Lowest Unoccupied Molecular Orbital), offers the possibility of evaluating the electronic reactivity and chemical stability of the artemisinin molecule.

parameter	**Artemisinin (gas eV)**	**Artemisinin (water eV)**
HOMO	*-7,33*	*-7,44*
LUMO	*-0,50*	*-0,59*

Table 8-IV: HOMO-LUMO of artemisinin

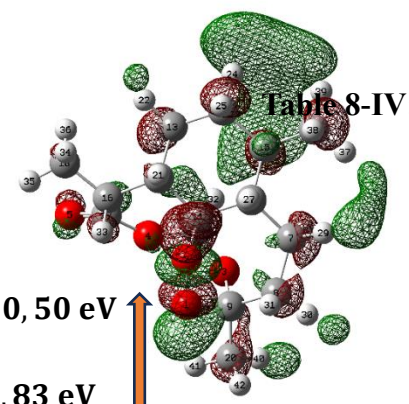

$\mathbf{E_{LUMO} = -0,50\ eV}$

$\mathbf{\Delta E = 6,83\ eV}$

$\mathbf{E_{HUMO} = -7,33\ eV}$

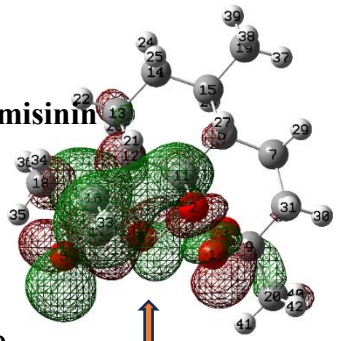

$\mathbf{E_{LUMO} =}$

$\boldsymbol{\Delta E = 6{,}85\ eV}$

$\mathbf{E_{HUMO} = -7,44\ eV}$

Figure VI-21: HOM-LUMO (artemisinin*)* in Gas phase

Figure VI-22: HOM-LUMO (artemisinin*)* in aqueous phase

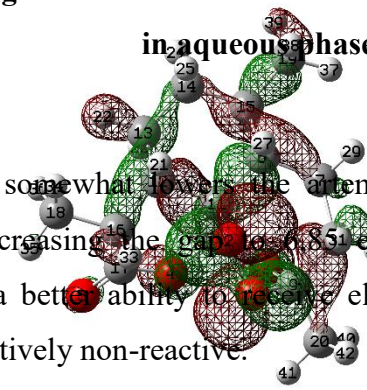

In comparison to the gas phase, the aqueous solvent somewhat lowers the artemisinin's HOMO (-7,44 eV) and LUMO (-0,59 eV) levels, increasing the gap to 6,85 eV. This stabilization, particularly of the LUMO, demonstrates a better ability to receive electrons, promoting its biological interactions while remaining relatively non-reactive.

The increase in the HOMO-LUMO energy difference in aqueous solution indicates an enhanced polarization of the molecule in polar environments, thus stimulating its chemical reactivity.

7. Structure-property relationship

The study of the structure of the artemisinin molecule via geometric optimization, as well as the analysis of its electronic and vibrational properties, reveals significant correlations between its molecular configuration and its chemical and biological characteristics.

7.1 Influence of geometry on responsiveness

Artemisinin has a tricyclic structure that includes an endoperoxide (O–O) bridge, The stability of this function, perceived as the active site of the molecule, is directly affected by the bond angle and the distance between the atoms of the peroxide ring.

7.2 Boundary orbital localization

Visualization of the HOMO and LUMO orbitals reveals that:

- ❖ HOMO is mainly located on the carbon skeleton and oxygen groups,

- While the LUMO is concentrated around the peroxide bridge.

This distribution suggests that electronic attack (reduction) occurs preferentially on this functional group, confirming its role in biological activity.

7.3 Correlation between polarity and activity

The dipole moment of the molecule increases in solution (table2-IV), indicating a greater polarization of the structure in aqueous medium. This enhances the ability of artemisinin to interact with polar biological targets, particularly in the parasite's intracellular environment.

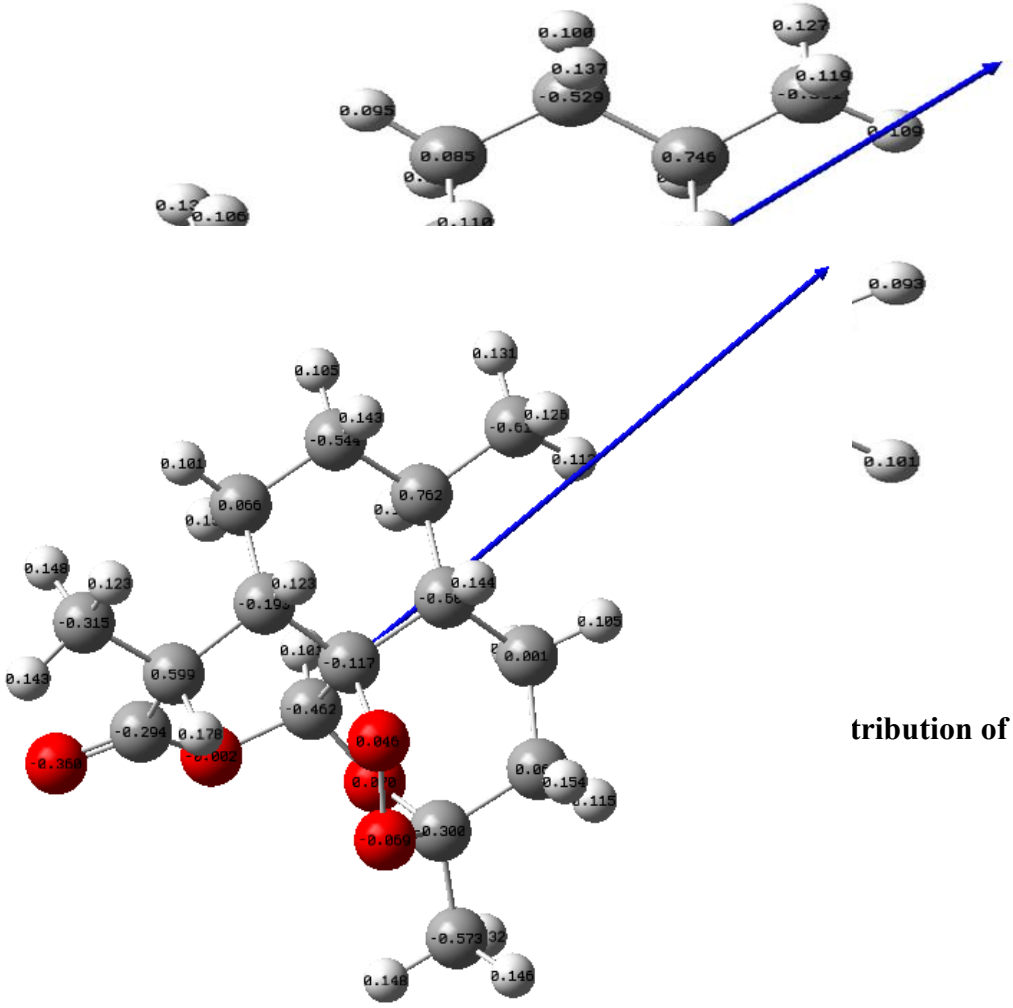

tribution of charge (Gas)

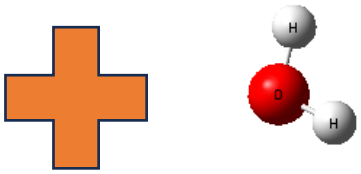

Figure VI-24: Distribution of charge (water*)*

7.4 HOMO–LUMO gap and stability

Finally, the shrinking of the HOMO–LUMO gap in an aqueous medium is in agreement with the increase in the chemical reactivity of the molecule. This indicates that the structure of artemisinin is finely adapted to its pharmacological role:

stable outside the body, but activatable under specific physiological conditions.

These results indicate that the therapeutic efficacy of artemisinin is closely associated with its three-dimensional (3D) structure and electronic properties. The structure-property relationship illustrates how the molecule is elaborated at the atomic level.

Part II: Results and discussion of glucose

1. Optimized molecular geometry

The DFT/B3LYP/6-31G++ (d', p') method was used for the geometric optimization of glucose in two different environments: in the gas phase and in the aqueous phase.

File type	.chk
Calculation type	Final OPT
Calculation method	RB3LYP
Basis set	6-31G++ (d', P')
Charge	0
Spin	Singlet
Solvation	None
Electronic Energy	-18700,42024 eV
RMS Gradient Norm	-7,89× 10^{-4} $eV/Bohr$
Dipole moment	2,535915 Debye
Imaginary freq	

Table 9-VI:Summary of glucose in gas phase

File type	.chk
Calculation type	Final OPT
Calculation method	RB3LYP
Basis set	6-31++ (d',p')
Charge	0
Spin	Singlet
Solvation	Scrf=solvent=water
Electronic Energy	-18700,97054 eV
RMS Gradient Norm	-3× 10^{-4} eV $/Bohr$
Dipole moment	3,483145 Debye
Imaginary freq	

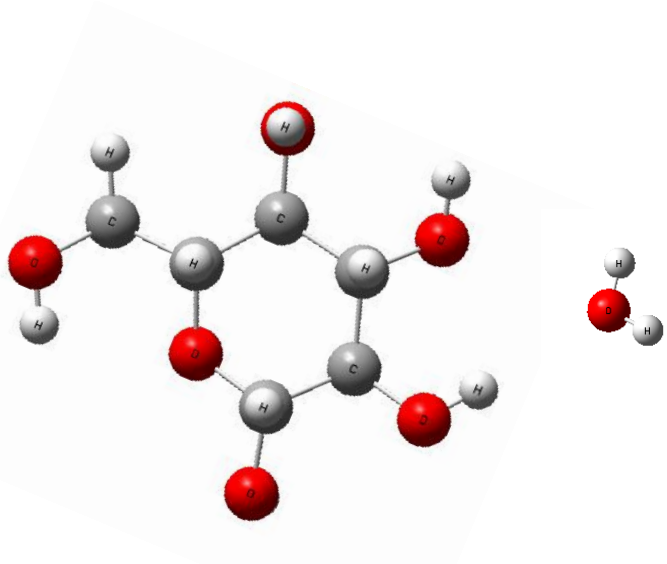

Figure VI-26: Glucose optimization in aqueous phase

Table 10-VI: Summary of glucose in aqueous phas

2. Electronic properties

The glucose's electrostatic potential (ESP) reveals a strongly polarized surface with areas that are electrophilic and linked to hydroxylated $(O-H)$,oxygens (O). This polarity encourages hydrogen bonding, which explains its high solubility and reactivity in biological systems.

Electrophilic site

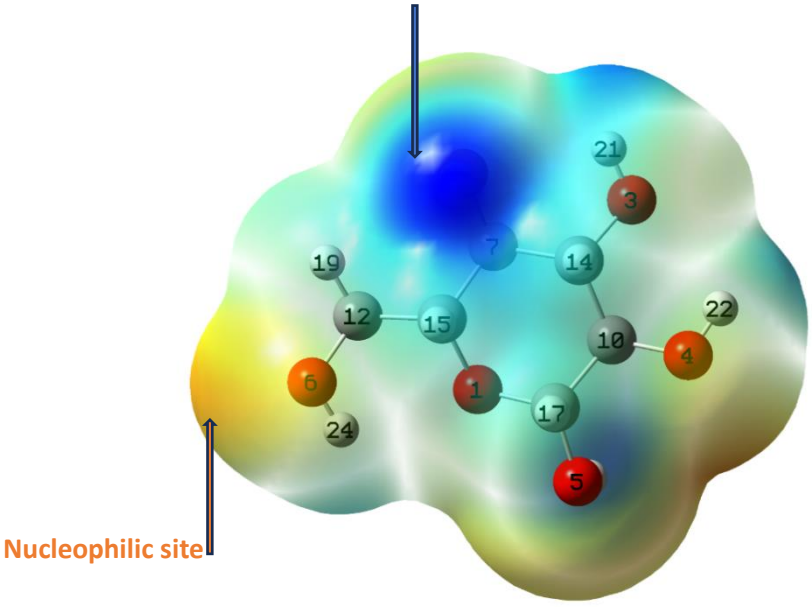

Figure VI-27: Electrostatic Potential (ESP) of glucose

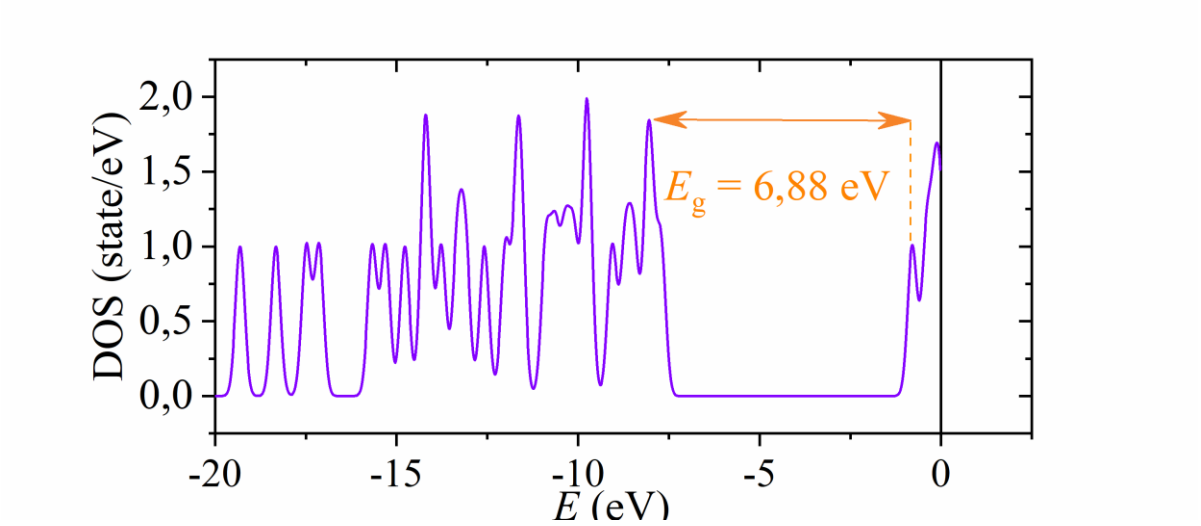

Figure VI-28: Density of states DOS (glucose)

HOMO

The Density Of electronic states (DOS) of glucose reveals a narrow separation between the HOMO and LUMO, indicating good electronic stability. The profile of DOS in aqueous solution shows a little compression of energy levels and an increase in electronic affinity, suggesting altered reactivity in a biological environment.

LUMO

parameter	Glucose (Gas eV)	Glucose (water eV)

Energy of the gap $E_{gap} = E_{LUMO} - E_{HUMO}$	6,85	6,88
Ionization Energy $E_i = -E_{HUMO}$	7,36	7,47
Electron Affinity $E_A = -E_{LUMO}$	0,51	0,59
Electronegativity $\chi = -\frac{(E_{HOMO} + E_{LUMO})}{2}$	3,93	4,03
Chemical Potential $\mu = \frac{(E_{HOMO} + E_{LUMO})}{2}$	-3,93	-4,03
Chemical Hardness $\eta = \frac{(E_{HOMO} - E_{LUMO})}{2}$	-3,43	-3,44
Chemical Softness $S = \frac{1}{\eta}$	-0,29	-0,29
Electrophilicity Index $\omega = \frac{\mu^2}{2\eta}$	2,26	2,36
Nucleophilicity Index $\varepsilon = \frac{1}{\omega}$	0,44	0,42

Table 11-VI: Global parameter (Glucose)

Despite a slight electronic polarization, glucose maintains a considerable global stability. An increase in electronic affinity and electrophilic index is observed in aqueous solution, indicating an increased ability to receive electrons. This evolution suggests a moderate level of reactivity that is better suited to interactions in a biological environment.

3. HOMO-LUMO energy gap and implications for reactivity

parameter	Glucose (gas eV)	Glucose (water eV)
HOMO	-7,36	-7,47
LUMO	-0,51	-0,59

Table 12-VI: HOMO-LUMO of Glucose

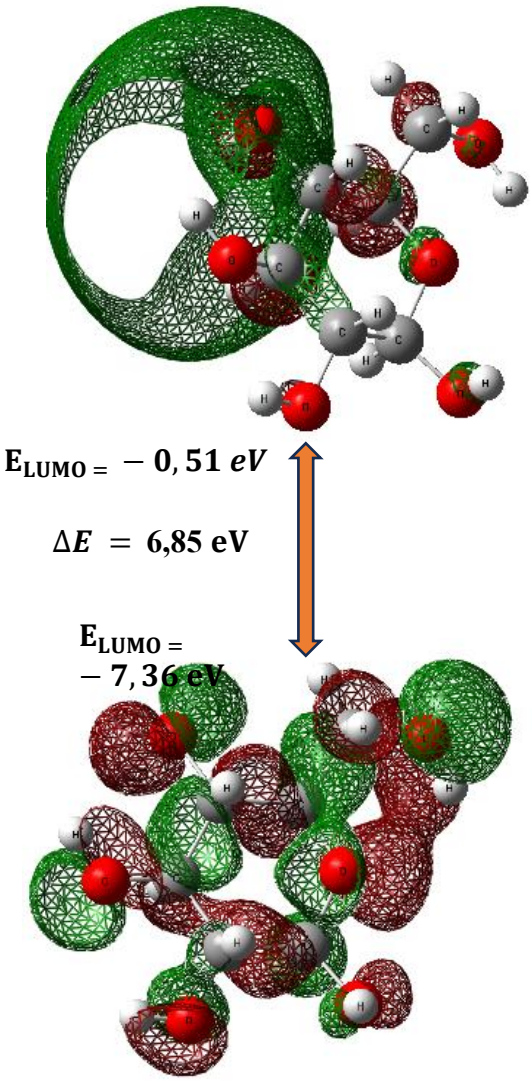

Figure VI -29: HOMO-LUMO Glucose in gas phase

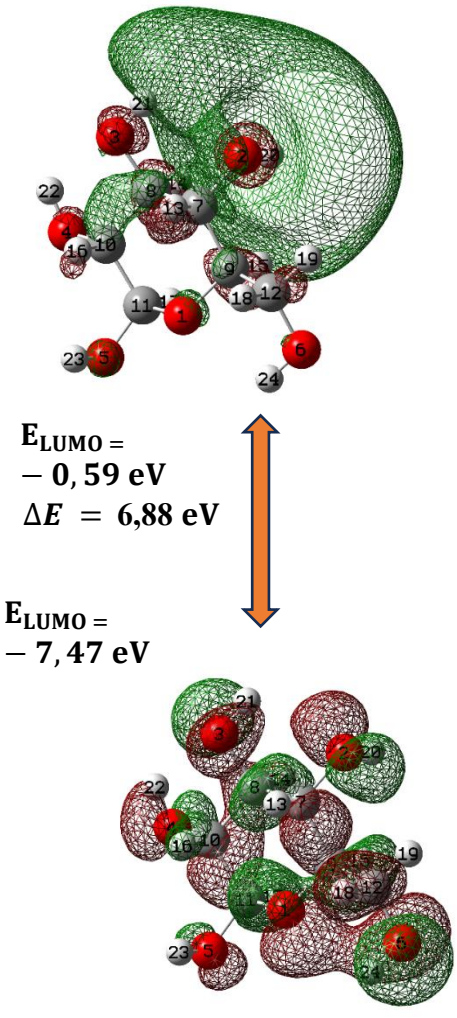

Figure VI-30: HOMO-LUMO Glucose in aqueous phase

In comparison to the gas phase, the aqueous solvent somewhat lowers the glucose's HOMO (-7,47 eV) and LUMO (-0,59 eV) levels, increasing the gap to 6,88 eV. This stabilization, particularly of the LUMO, demonstrates a better ability to receive electrons, promoting its biological interactions while remaining relatively non-reactive.

The increase in the HOMO-LUMO energy difference in aqueous solution indicates an enhanced polarization of the molecule in polar environments, thus stimulating its chemical reactivity.

Part **III: Results and discussion of interaction artemisinin-glucose complex**

1. Optimized molecular geometry

The DFT/B3LYP/3-21G method was used for the geometric optimization of artemisinin-glucose complex in two different environments: in the gas phase and in the aqueous phase.

File type	**.chk**
Calculation type	**Final OPT**
Calculation method	**RB3LYP**
Basis set	**3-21G**
Charge	**0**
Spin	**Singlet**
Solvation	**None**
Electronic Energy	**-3784,069802 eV**
RMS Gradient Norm	**1,36 × 10^{-4} $eV/Bohr$**
Dipole moment	**14,627826 Debye**
Imaginary freq	

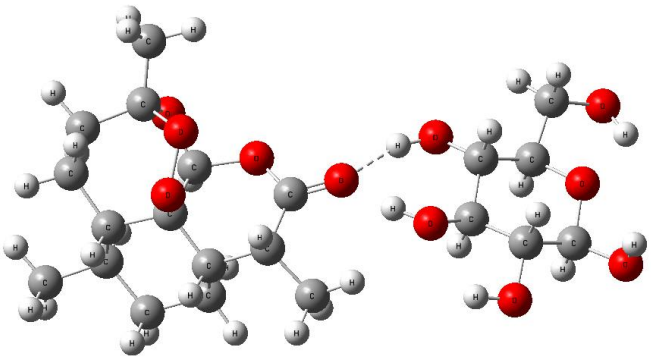

Figure VI-31: Artemisinin-Glucose complex optimization in gas phase

Table 13-VI: summary artemisinin-glucose complex in gas phase

File type	**.chk**
Calculation type	**Final OPT**
Calculation method	**RB3LYP**
Basis set	**3-21G**
Charge	**0**
Spin	**Singlet**
Solvation	**Scrf=solvent=water**
Electronic Energy	**-44601,90603 eV**
RMS Gradient Norm	**4,35× 10^{-4} $eV/Bohr$**
Dipole moment	**16,991752 Debye**
Imaginary freq	

Table 14-IV: summary artemisinin-glucose complex in aqueous phase

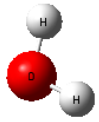

Figure VI-32: Artemisinin-glucose optimization complex in aqueous phase

2. Structural analysis

In this section, there is Compare the optimized structure of the artemisinin-glucose complex with that of the isolated molecules (artemisinin and glucose*)* in the aqueous phase.

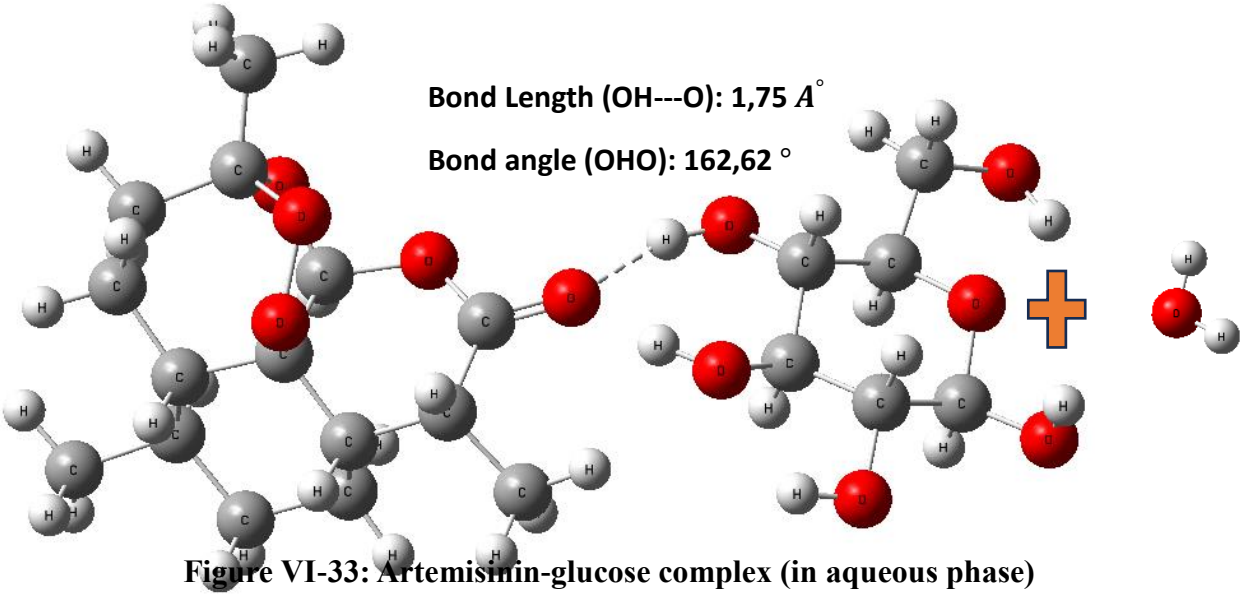

Figure VI-33: Artemisinin-glucose complex (in aqueous phase)

Parameters	Artemisinin (water)	Glucose (water)	Artemisinin-Glucose (water)
Bond lengths			
$O_1 - O_2$	$1,459\ A^\circ$		$1,525\ A^\circ$
$O_2 - C_{11}$	$1,464\ A^\circ$		$1,507\ A^\circ$
$C_{11} - C_{12}$	$1,540\ A^\circ$		$1,536\ A^\circ$
$O_2 - H_{20}$		$0,96\ A^\circ$	
$C_9 - O_1$		$1,43\ A^\circ$	
$C_{12} - H_{19}$		$1,09\ A^\circ$	
$C_8 - C_{10}$(Ring)		$110,15^\circ$ $1,10\ A^\circ$	
Bond angles			
$O_2 - O_1 - C_9$	$108,941^\circ$		$106,054^\circ$
$O_2 - C_{11} - C_{12}$	$106,30\,0^\circ$		$103,744^\circ$
$C_6 - C_{11} - C_{12}$	$112,87^\circ$		$113,428^\circ$
$C_8 - C_{10} - C_{11}$(ring)		$110,15^\circ$	
$C_7 - C_9 - O_1$(ring)		$109,47^\circ$	
$C - 0 - H$		107°	
$H - C - H$		$108,52^\circ$	
Dihedral angles			
$O_2 - O_1 - C_9 - O_3$	$-73,876^\circ$		$-76,956^\circ$
$C_{10} - O_3 - C_9 - O_1$	$35,115^\circ$		$34,944^\circ$
$O_3 - C_8 - C_{10} - O_4$		$63,77^\circ$	$58,03^\circ$
$C_8 - C_{10} - C_{11} - O_1$		$55,82^\circ$	$60,43^\circ$
$C_{12} - C_9 - C_7 - O_2$		$62,79^\circ$	$66,44^\circ$
$C_8 - C_{10} - C_{11} - O_5$		176°	$179,93^\circ$

Table 15-IV: Rearrangement of (bond lengths, angles and dihedral)

A strong hydrogen bond with a clear orientation (**1,75 A° , 162,62°**) in the artemisinin–glucose complex results in a stable donor-acceptor interaction. A favorable polarization and conformational adaptation are shown by changes in lengths, angles, and dihedrals. These components verify that a stable and active complex has formed in an aquatic environment.

3. Molecular energy levels (Homo–Lumo)

Parameter	Artemisinin (water) eV	Glucose (water) eV	Artemisinin-Glucose eV (water)
HOMO	**-7,44**	**-7,47**	**-6,55**
LUMO	**-0,59**	**-0,59**	**-0,89**
Energy of gap	**6,85**	**6,88**	**5,66**

Table 16-IV: HOMO-LUMO of artemisinin-glucose complex

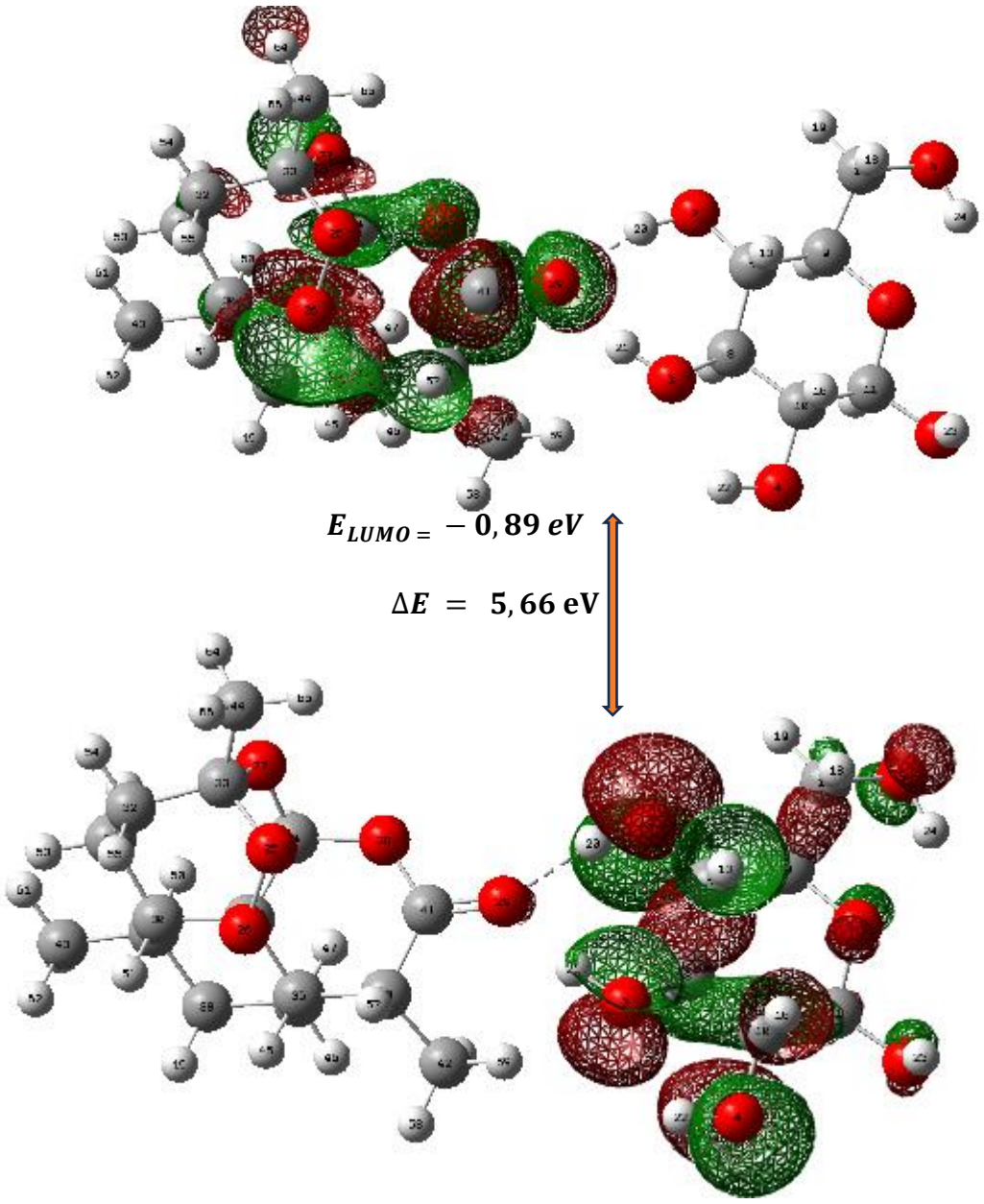

Figure VI -34:HOMO-LUMO artemisinin-glucose complex in aqueous phase

In the artemisinin–glucose complex, the elevation of the HOMO level (-6,55 eV) and the decrease of the LUMO (-0.89 eV) result in an electronic reorganization caused by hydrogen bonds. This configuration suggests a system's increased stability and maybe strengthened electronic reactivity in biology environment.

4. Electronic load distribution (MULLIKEN analysis)

The Mulliken charge analysis reveals polarization effects and charge transfer events that affect molecule stability and reactivity, offering insights into the electronic load distribution inside the artemisinin–glucose complex.

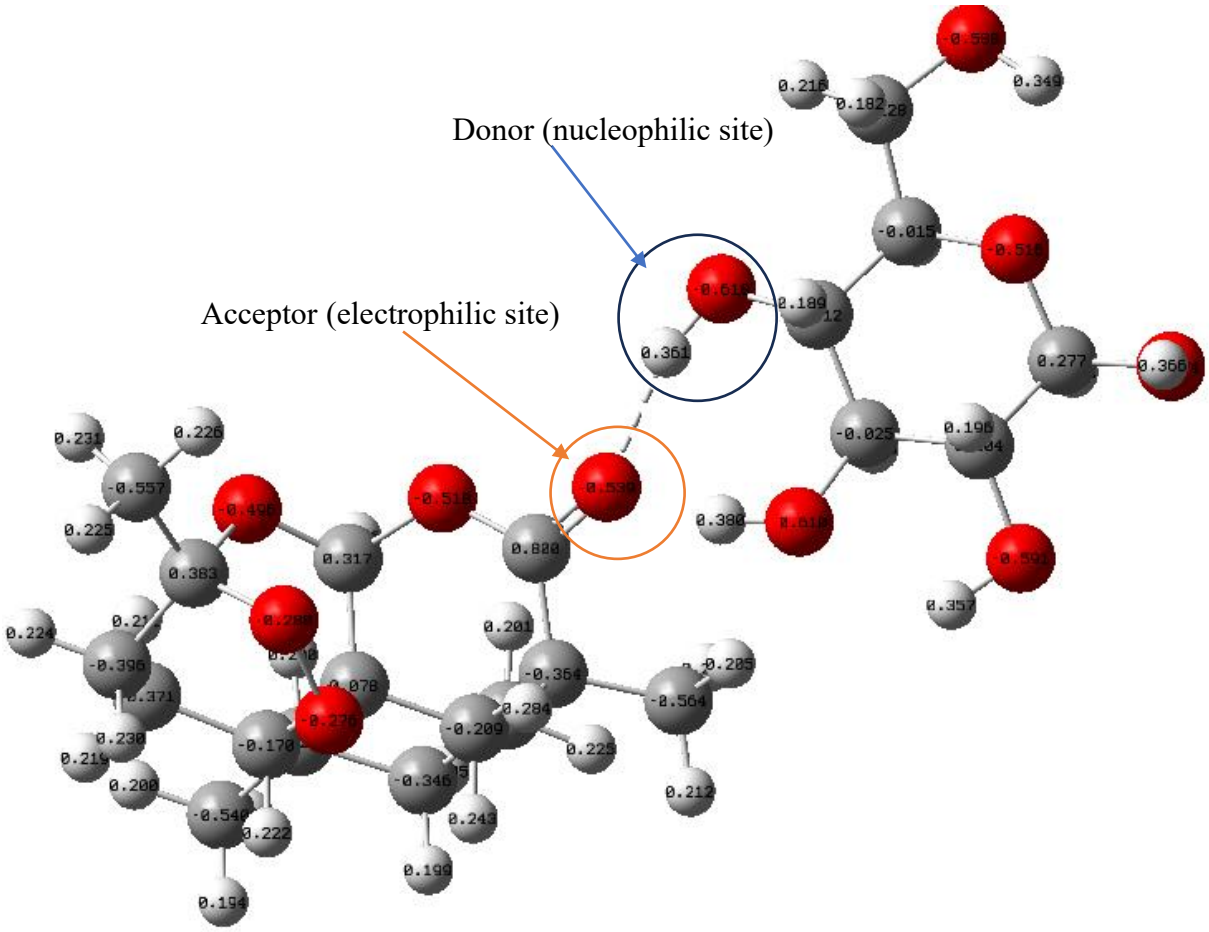

Figure VI-35:Distribution of charge (artemisinin-glucose complex)

A stable hydrogen bond and an electronic polarization are revealed by the charge distribution in the artemisinin–glucose complex. Glucose acts as an electron donor, while artemisinin acts as an acceptor. This donor-acceptor interaction causes an electronic density redistribution, strengthening the complex's stability in a biological environment.

5. Effect of the solvent and energy of interaction

We compare artemisinin and glucose molecules isolated with artemisinin-glucose complex in the phase gazeuse with the study conducted in the presence of a solvent (such as water) in this section.

Molecule	Gas eV	Water eV
Artemisinin	-26062,05873	-26148,96689
Glucose	-18700,42024	-18700,97054
Artemisinin-Glucose	-3784,069802	-44601,90603

Table 17-VI: Electronic energy

- Calculates of interaction energy

$$\Delta E_{interaction} = E_{Art-Glc} - (E_{artemisinin} + E_{glucose}) \qquad (IV\text{-}27)$$

$\Delta E_{int-gas}$= **(-3784,069802-(-26062,05873-18700,42024))×23,06 = 944962,1154** $kcal/mol$

$\Delta E_{int-water}$= **(-44601,90603-(-26148,96689-18700,97054))×23,06 = 5719,6041** $kcal/mol$

$$\Delta E_{int-gas} >> \Delta E_{int-water}$$

The complex (artemisinin-glucose) is stabilized via interactions with the solvent, as evidenced by the lower liaison energy in the aqueous phase. It implies greater stability and increased compatibility with the biological environment**.**

Part IV: Results and discussion of interaction artemisinin and Fe^{2+}

In addition to its traditional uses in reducing blood sugar levels, another, more common use of artemisinin is in the treatment of malaria. Malaria is one of the most common and deadly diseases in the world. Malaria is caused by the Plasmodium falciparum parasite, which has the ability to reproduce rapidly and is transmitted to humans through the bite of female Anopheles mosquitoes. This disease causes symptoms similar to those of influenza and severe anemia. The number of malaria cases in 2023 reached 263 million. Most of these cases occurred in Africa, particularly sub-Saharan Africa.

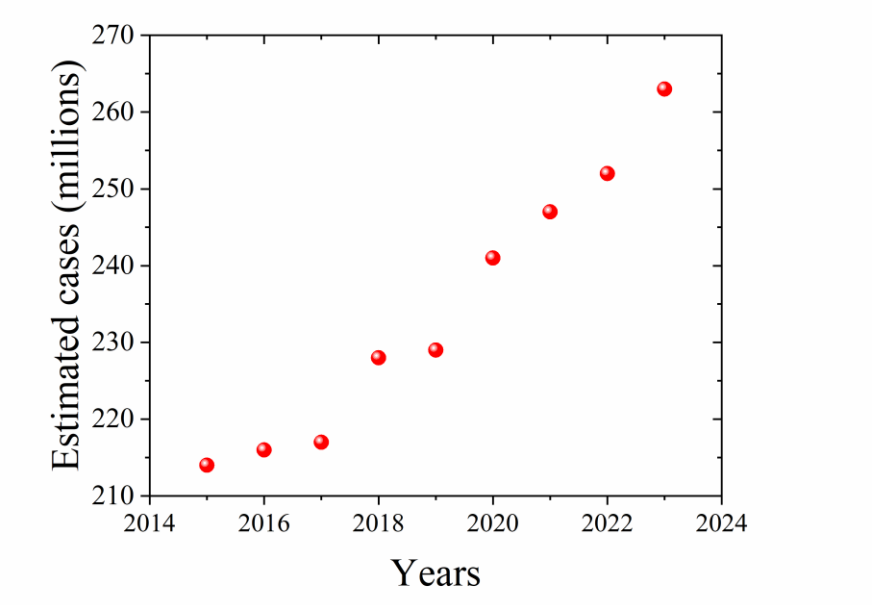

Figure IV-36: Number of malaria cases from 2015 to 2023

Artemisia annua has been used for centuries to treat this disease, and the artemisinin molecule is considered the primary agent in the treatment of malaria. However, due to its limited bioavailability, other artemisinin derivatives are being developed to improve the pharmacological properties of artemisinin, such as dihydroartemisinin and artesunate, all of which are highly absorbed compounds in the human mouth or in the intestinal mucosa. After being absorbed, artemisinin enters the blood, where it selectively binds to red blood cells infected with malaria parasites. Artemisinin's selectivity in targeting malaria-infected red blood cells stems from abnormalities in the cell membrane of infected blood cells, which allow larger quantities of artemisinin molecules to penetrate these cells compared to healthy cells [The parasitophorous vacuole nutrient channel is critical for drug access in malaria parasites and modulates the artemisinin resistance fitness cost]. In addition, artemisinin can also cross the blood-brain barrier with low toxicity [Artemisinin Attenuates Amyloid-Induced Brain Inflammation and Memory Impairments by Modulating TLR4/NF-κB Signaling]. Upon

entering red blood cells, artemisinin interacts with iron (II), or heme, abundant within malaria-infected red blood cells. The high availability of iron (II) within malaria-infected blood cells is due to the malaria parasite's consumption of large quantities of hemoglobin and the release of large quantities of iron (II). The interaction between artemisinin and iron (II) leads to the cleavage of the anhydroxide bridge, generating highly toxic free radicals such as oxygen radicals and carbon radicals. These radicals target various proteins of the malaria parasite as well as fatty acids in the parasite's membranes, destroying its membrane structure.Using molecular simulations, we studied the reaction between Fe^{2+} and an artemisinin molecule. We calculated the energy of both the $Fe^{2+}$and the artemisinin molecule. We then calculated the energies of the products that might result from the reaction between the iron atom and the artemisinin molecule. The calculation results showed that the energy of the products is lower than the energy of the reactants, which means that the iron-artemisinin complex tends to dissociate into other products, including the Fe^{3+}, which may react with other artemisinin molecules inside the red blood cells.

$$\Delta E = E_{Products} - E_{Reactants} = -2001{,}94 \text{ eV}$$

The ozone molecule O_3 may dissociate into oxygen atoms, releasing heat and a hydroxyl radical OH^-. Hydroxyl radicals have been shown to be highly toxic to malaria parasites, and increasing the concentration of these radicals ultimately leads to the destruction of the

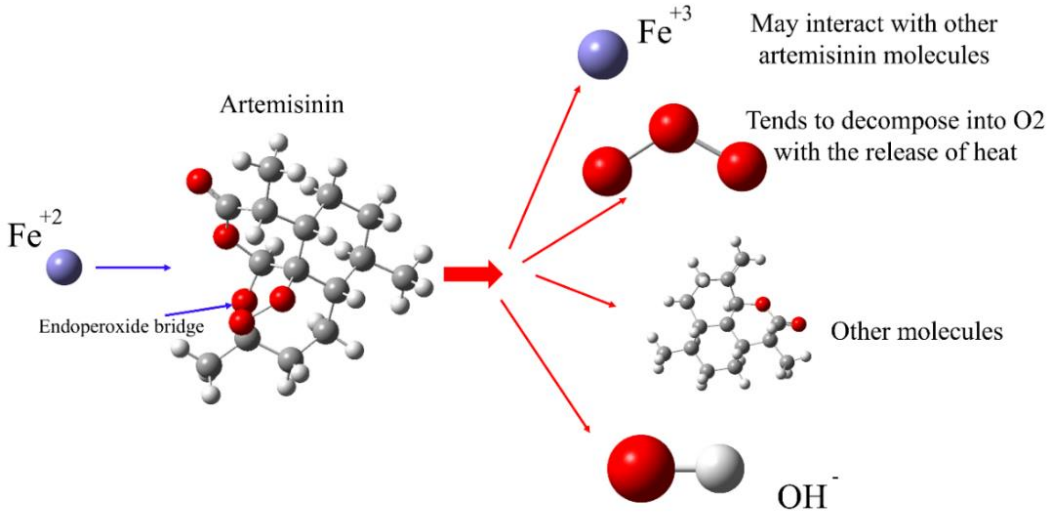

parasite.

Figure IV-37: The interaction between artemisinin and Fe^{2+}

Conclusion

In conclusion analysis of the artemisinin-glucose complex revealed the formation of significant non-covalent interactions, including stabilizing hydrogen bonds, and artemisinin acts directly with glucose to reduce its electronic density, which confirms its hypoglycemic effect. In the other hand molecular simulations indicate that the reaction between Fe^{2+} and artemisinin is energetically favorable, with a significant energy release ($\Delta E = -2001{,}94$ eV), suggesting spontaneous dissociation into products such as Fe^{3+}, O_3 and other fragments These products may further react within red blood cells. Additionally, the generation of reactive species like hydroxyl radicals (OH^-) from ozone dissociation could enhance the antimalarial effect by contributing to the destruction of malaria parasites.

GENERAL CONCLUSION

General conclusion

The objective of this work was to study the structural and vibrational properties of the artemisinin molecule in order to deepen our understanding of its pharmacological actions, including its antimalarial and hypoglycemic effects.Using density functional theory (DFT), we were able to accurately determine the electronic structure of artemisinin and its molecular interactions with two important biological targets: iron (II) (Fe^{2+}) on one side, and glucose on the other.

The study of the artemisinin-glucose complex revealed the formation of significant non-covalent interactions, including stabilizing hydrogen bonds. This structural affinity indicates that artemisinin may interact directly with glucose, raising the possibility of its involvement in regulating blood sugar levels. These results provide additional insight into recent pharmacological studies that have observed a hypoglycemic effect in certain animal models.

In parallel, analysis of the artemisinin–Fe^{2+} complex revealed a potential activation of the molecule by breaking the peroxide bond, a process essential for its antimalarial effect. This interaction is consistent with experimental data indicating the production of reactive species capable of causing irreversible damage to the parasite's biomolecules.Thus, our research supports the idea that artemisinin has many therapeutic possibilities, beyond its well-defined role in the fight against malaria.

In perspective, the findings of this research call for the implementation of additional experimental studies, both in vitro and in vivo, to confirm the interactions revealed by modeling and to examine in more detail the potential role of artemisinin in the regulation of metabolic disorders, including type 2 diabetes. In addition, the use of this approach on other artemisinin derivatives could promote the development of new pharmacological entities with a dual action, both against malaria and hypoglycemic.